

ENSO, IOD, SST: IMPACT STUDY ON NEMR IN  
TAMIL NADU, SOUTH INDIA

By

Mahalakshmi Bargavi Govindasamy Thulasi

A THESIS

Submitted to

Michigan State University

in partial fulfillment of the requirements

for the degree of

MASTER OF SCIENCE

GEOGRAPHY

2011

## **ABSTRACT**

ENSO, IOD, SST: IMPACT STUDY ON NEMR IN TAMIL NADU, SOUTH INDIA

By

Mahalakshmi Bargavi Govindasamy Thulasi

Rainfall variability in Tamil Nadu, a southeastern state in India, is gaining importance for its associations with ocean-atmosphere coupled phenomena such as the El-Niño Southern Oscillation (ENSO) and the Indian Ocean Dipole (IOD) mode. These rainfall patterns are also driven by surface latent heat flux (SLHF), Sea Surface Temperature (SST), Water Vapor content observed over the Indian Ocean, especially coincident with the 2004 earthquake in Sumatra. This study analyzes rainfall characteristics for Tamil Nadu during the north-east monsoon rainfall (NEMR) period starting from October through December over the period of 1982 - 2005. In particular, this study examines the relationship between the SST change in - the Nino regions, Saji regions and the 2004 Earthquake epicenter region - and rainfall variations in Tamil Nadu. This can improve understanding of global remotely sensed variables (e.g. precipitation, SST) and in applications such as climate modeling. This would lead to the comprehension and thus, a complete documentation of the rainfall pattern in this region that would help us understand its behavior with respect to other climate factors related to moisture transport.

Keywords: NEMR, IOD, ENSO, SST

**“India as a whole is too large to be treated as a single unit”**

- Sir Charles Normand  
(Monsoon Seasonal Forecasting, 1953)

Dedicated to **my parents** who have sacrificed their comforts and worked hard allowing me and my sisters to enjoy the opportunities they missed.

## ACKNOWLEDGEMENTS

Firstly, I would like to thank my advisor Dr. Nathan Moore who has guided me all through my thesis and research work and has supported and encouraged me in each step of my progress in both my academic and professional life. Secondly, I would like to extend my thanks to my committee members Dr. Jiaguo Qi and Dr. Lifeng Luo who have continued to let me experiment my work and provided valuable suggestions throughout my work. I owe a sincere thanks to Dr. Jiaguo Qi for having offered an office space in CGCEO allowing me to work in the research projects and my thesis in the center. Also, I would like to thank the Geography department for having provided funding in the form of Teaching Assistantship and an office space throughout my two years of graduate life and has permitted me to use all the resources available in the department. I have learnt and continue to learn a lot from Geography faculty and students ever since August 2009 and would like to appreciate their efforts in allowing me to expand my knowledge in Geo-spatial technologies and gain proficiency in the same.

Certainly, my graduate study and this thesis work would not have been possible if it was not for the support provided by my parents – Thank you Mom and Dad for your confidence in me. Further, I extend my thanks to my sisters – Kala, Manju and Beenu - who have constantly encouraged me in each step of my life. In addition, I thank Kristie who has been a great friend since the start of my graduate program and has been with me always. Thanks to my Indian friends who have made me not miss India and my family a lot since August 2009. Last but not the least, my work and life would have been incomplete without the presence of Sathya who continuously furthered my confidence and helped me stay cool. Thank you Sathya for being with me.

# TABLE OF CONTENTS

LIST OF TABLES .....	viii
LIST OF FIGURES .....	ix
CHAPTER 1 .....	1
INTRODUCTION .....	1
1.1 An Overview.....	1
1.2 Background.....	2
1.3 Research Questions.....	5
1.4 Research Goals .....	6
1.5 Hypotheses.....	7
1.6 Research Need .....	9
1.7 Research Relevance.....	13
CHAPTER 2 .....	14
LITERATURE REVIEW .....	14
2.1 Monsoon Forecast – An Overview .....	14
2.2 ENSO.....	15
2.2.1 ENSO and SOI – An Overview .....	15
2.2.2 Niño Regions and SST.....	17
2.2.3 ENSO and Indian Monsoon .....	20
2.3 IOD .....	21
2.3.1 IOD and DMI – An Overview .....	21
2.3.2 ENSO & IOD Interactions .....	24
2.3.2 IOD and Indian Monsoon .....	25
2.4 Sumatra-Andaman Earthquake – An Overview .....	26
2.4.1 Slip Process .....	26
2.4.2 Precursors to an earthquake.....	29
CHAPTER 3 .....	32
STUDY REGIONS, DATA AND METHODOLOGY .....	32
3.1 An Overview.....	32
3.1.1 Tamil Nadu.....	32
3.1.2 Sea Surface Temperature Regions .....	33
3.2 Datasets.....	35
3.2.1 Rainfall .....	35
3.2.2 Sea Surface Temperature.....	36
3.2.3 Southern Oscillation Index .....	37
3.2.4 Dipole Mode Index.....	37
3.3 Methodology.....	38
3.3.1 Rainfall Domains.....	38
3.3.2 Time Series Analysis & Analysis of Variance .....	38
3.3.3 Time-lag Correlation .....	39

3.3.4	Principal Component Analysis and Regression model .....	40
CHAPTER 4 .....		43
RESULTS AND ANALYSIS.....		43
4.1	Rainfall Domains in Tamil Nadu.....	43
4.2	Time Series Analysis & Analysis of Variance .....	50
4.2.1	Rainfall Pattern.....	50
4.2.2	SST Pattern.....	56
4.2.3	SOI Pattern .....	67
4.2.4	DMI Pattern .....	69
4.3	Time-lag Correlation .....	71
4.3.1	Rainfall Domain – TN East .....	71
4.3.2	Rainfall Domain – TN North & South .....	73
4.4	Principal Component Analysis and Regression model.....	74
CHAPTER 5 .....		78
DISCUSSION .....		78
5.1	Time Series Analysis .....	78
5.2	Time-lag Correlation .....	79
5.3	Principal Component Analysis and Regression model.....	81
5.4	Limitations.....	82
CHAPTER 6 .....		84
CONCLUSIONS.....		84
6.1	Conclusions .....	84
APPENDICES .....		86
R PROGRAMS.....		87
REFERENCES .....		93

## LIST OF TABLES

Table 2.1 Niño Regions .....	18
Table 4.1 Descriptive statistics of annual rainfall variation for the 24 year study period .....	42
Table 4.2. Rainfall variation of the four domains in Tamil Nadu based on 24-year mean rainfall .....	47
Table 4.3 Pair wise comparisons of Rainfall Variations across all domains in Tamil Nadu.....	46
Table 4.4 Pair wise comparisons of Rainfall Variations across the final domains in Tamil Nadu .....	48
Table 4.5 Inter Quartile Range (IQR) values for rainfall domains in Tamil Nadu.....	554
Table 4.6 Pair wise comparisons of SST Variations across all regions (1982 – 2005) .....	576
Table 4.7 Time-lag Correlation matrices for TN East Rainfall Domain (a) October rainfall (b) November rainfall (December rainfall) .....	71
Table 4.8 Time-lag Correlation matrices for TN West Rainfall Domain (a) October rainfall (b) November rainfall (December rainfall) .....	72
Table 4.9 Component Loadings for TN East Domain .....	74
Table 4.10 Variance explained by the first three components in TN East Domain (a) Total Variance explained (b) Percentage of Variance explained .....	74
Table 4.11 Component Loadings for TN West Domain.....	74
Table 4.12 Variance explained by the first three components in TN West Domain (a) Total Variance explained (b) Percentage of Variance explained .....	75

## LIST OF FIGURES

Figure1.1 South Eastern state of India - ‘Tamil Nadu’ (highlighted).....	3
Figure 1.2: November 2005 Rainfall in Chennai (recorded value: 215mm in 24 hours); (a) & (b) illustrate the damage and costs brought about by 2005’ aggressive rainfall .....	10
Figure1.3: November 2008 Rainfall in Chennai (recorded value of monthly rainfall: 556 mm); (a) & (b) illustrate flooding occurrence in the residential areas of Chennai metropolitan area caused by 2008’ downpour. ....	11
Figure1.4: Precipitation Anomaly during NEMR period for the cities of Chennai, Namakkal and Pondicherry with a main focus on the recent decades (1990 – 2008). ....	12
Figure2.1 Niño Regions (source: www.cpc.noaa.gov).....	18
Figure2.2 Dipole Events (a) Positive Dipole Event (b) Negative Dipole Event .....	23
Figure2.3 Sub-division of the earthquake rupture zone into Sumatra segment, Nicobar segment and Andaman segment (Lay et. al., 2005) .....	28
Figure2.4 Surface Latent Heat Anomaly – 07 December 2004 (Singh et al., 2007).....	30
Figure3.1: Sea Surface Temperature (SST) regions .....	34
Figure4.1: 24-Years Mean Annual Rainfall Variation in Tamil Nadu - Entire state.....	45
Figure4.2: 24-Years Mean Annual Rainfall Variation in Tamil Nadu - Domains highlighted ....	46
Figure4.3: Box plots of Rainfall Variations across all domains in Tamil Nadu.....	48
Figure4.4: Box plots of Rainfall Variations across the final domains in Tamil Nadu.....	49
Figure4.5: Time Series plots of Monthly Rainfall Variations for the period 1982 – 2005 (a) TN East Domain (b) TN West Domain.....	51
Figure4.6: Box plots of Monthly Rainfall Variations for the period 1982 – 2005 (a) TN East Domain (b) TN West Domain.....	53
Figure4.7: Box plot of SST Variations across all regions for the period 1982 – 2005.....	56
Figure4.8: Time Series plots of SST Variations for each region (1982 – 2005); (a) SST-1 region; (b) SST-2 region; (c) SST-3 region; (d) SST-4 region; (e) SST-5 region .....	57
Figure4.9: Box plots of SST Variations for each region (1982 – 2005); (a) SST-1 region; (b) SST-2 region; (c) SST-3 region; (d) SST-4 region; (e) SST-5 region.....	62
Figure4.10: Southern Oscillation Index Variation (1982 – 2005) (a) Time Series plot (b) Box plot .....	67
Figure4.11: Dipole Mode Index Variations (1982 – 2005) (a) Time Series plot (b) Box plot.....	69

# CHAPTER 1

## INTRODUCTION

### 1.1 An Overview

Rainfall variability in Tamil Nadu (TN), a southeastern state in India, is gaining importance for its associations with ocean-atmosphere coupled phenomena such as the El-Niño Southern Oscillation (ENSO) and the Indian Ocean Dipole (IOD) mode. A complete documentation of the rainfall pattern in this region is necessary to understand its behavior with respect to other climate factors related to moisture transport. These rainfall patterns are also driven by many ocean-atmosphere factors observed over the Indian Ocean, especially coincident with the disastrous earthquake of moment magnitude 9.3 that occurred on 26th December 2004 triggering gigantic tsunami waves.

The main objective of this study is to analyze the spatial and temporal variations of rainfall across TN over a period of 24 years (1982 to 2005) for the North-East Monsoon Rainfall (NEMR) period starting from October through December. In particular, this study examines the relationship between the Sea Surface Temperature (SST) anomaly related to the 2004 Earthquake triggered Tsunami and rainfall variations in Tamil Nadu, respectively. Additionally, possible causative factors including, El-Nino Southern Oscillation (ENSO), Indian Ocean Dipole (IOD), SST will be analyzed for the same period and area. This would facilitate to test the hypothesis if increase in SST values around earthquake prone zone in Sumatra in Indonesia, southeast Indian Ocean region, affects rainfall pattern in TN.

## 1.2 Background

The Indian monsoon highly depends on the ‘South-West Monsoon Rainfall (SWMR)’ period starting from June to September and the ‘North-East Monsoon Rainfall (NEMR)’ period starting from October to December. With varying topography in India, large amounts of rainfall are received during the SWMR period along the west coast and northern plains of India as compared to its north-eastern counterpart. This is due to convergence, orographic lift caused by Western Ghats and monsoon troughs and tropical depressions development respectively (Simpson et al., 2007). As mentioned by Kumar et al., (2004), there are three important stages associated with the monsoon changing period. These synoptic circulation stages observed with the onset of NEMR are: (1) the retreat of SWMR from India during September – October; (2) the reversal of lower level winds from South-Westerlies to North-Easterlies; and (3) an increase in rainfall over southern parts of India.

Recent research using model integrations has shown that summer South Asian monsoon is not sensitive to the heating of Tibetan Plateau instead its sensitive to the band of mountains south and west of the plateau. Further, a slight increase in precipitation was observed SouthWest of the Plateau and over the ocean near 15° N meaning that Tibetan Plateau heating shifts rainfall to the Himalayas. It has also been proved that Tibetan Plateau heating may be important for East Asian climate instead of South Asian monsoon as was originally thought (Boos and Kuang, 2010).

In contrast, the southeast coast of India lies in a rain shadow region during the SWMR period and does not receive as much rain as the rest of the country. As a result, NEMR plays a critical role in the agricultural activities over five main meteorological subdivisions, namely, coastal Andhra Pradesh, Rayalseema, south interior Karnataka, Kerala and Tamil Nadu (Figure 1;

Revadekar and Kulkarni, 2008). Thus, NEMR becomes very important especially when SWMR fails in southern part of the country.

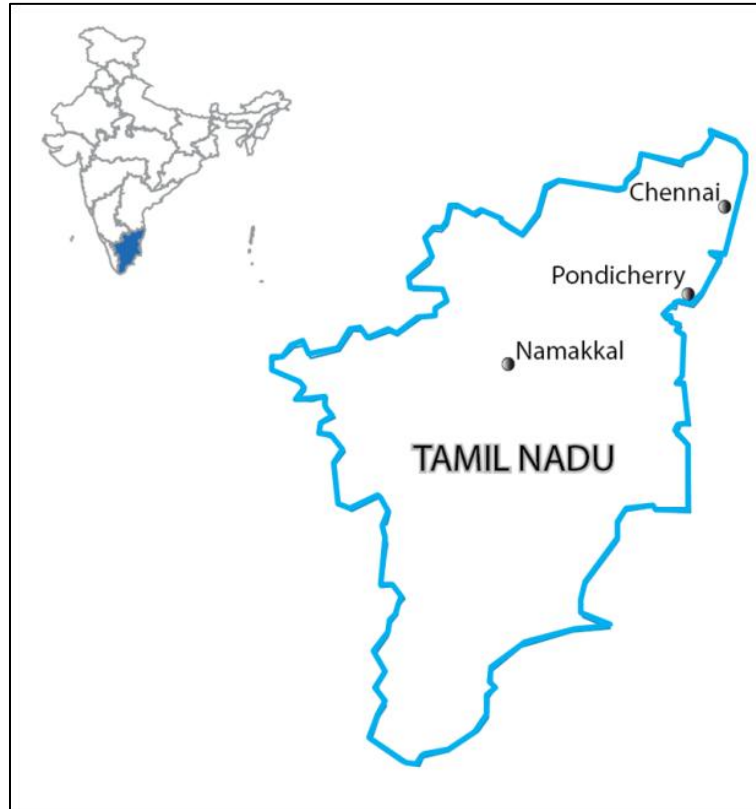


*Figure 1.1 South Eastern state of India - 'Tamil Nadu' (highlighted)*

(For interpretation of the references to color in this and all other figures, the reader is referred to the electronic version of this thesis)

Tamil Nadu (Latitude:  $8^{\circ} 5' N$  to  $13^{\circ} 35' N$ , Longitude:  $76^{\circ} 15' E$  and  $80^{\circ} 20' E$ ), a Southeastern state in India, receives less SWMR than other parts of the country and about 48% of the annual rainfall from the NEMR period (Regional Meteorological Centre, Chennai, India). Tamil Nadu is one of the many states affected by both the temporal and spatial variability of monsoon rainfall. Thus, NEMR affects both agriculture and economy in a very critical manner with its either delayed or early onset (Srinivasan and Ramamurthy, 1973).

Owing to its variability, the study of rainfall variability is of utmost importance and has been of high interest from early 20<sup>th</sup> century to present date. Research studies have identified a number of ocean-atmosphere coupled phenomena and other climate factors causing rainfall variability globally. The El-Niño Southern Oscillation (ENSO) is one of the major drivers of interannual variability in global rainfall (Normand, 1953; Haddad et al., 2004). In addition to ENSO, the Indian Ocean Dipole (IOD) mode is one of the major ocean-atmosphere-coupled phenomena in the tropical Indo-Pacific region (Saji et al., 1999; Webster et al., 1999). Several studies have examined the correlation between the Southern Oscillation Index (SOI) and the Indian summer monsoon rains (June through September) (Sikka, 1980; Rasmusson and Carpenter, 1983; Shukla and Paolina, 1983) and some studies have focused on ENSO and IOD during the NEMR period (Pant and Rupa Kumar, 1997; Geethalakshmi et al., 2009). However, these studies have concentrated mainly on Indian summer monsoon variability with less focus being given to NEMR in Tamil Nadu. Further, NEMR's variation over southern India, as a whole, lacks good documentation when compared to that of SWMR (Kripalini and Kumar, 2004). Therefore, it is worthwhile to examine NEMR's variation over this part of the country which lacks much attention.

In addition, research studies focused on identifying generic precursors to coastal earthquakes have observed high values in precipitation rate, Surface Latent Heat Flux (SLHF; it results from phase change of water due to solidification, evaporation or melting and it represents energy transport in the form of water vapor and heat between the earth's surface and atmosphere) and Sea Surface Temperature (SST) about 15 to 20 days prior to an eruption near the epicentral region (Dey and Singh, 2003; Chen et al., 2006; Singh et al., 2007). This is related to the Tsunami caused by a disastrous earthquake of moment magnitude 9.3 (epicenter: latitude: 3.30°

N, longitude: 96° E, depth: 30 km) off the coast of Sumatra on 26 December 2004 (Lay et. al, 2005). Although, epicentral regions have been studied in detail, countries neighboring such an epicenter have been lacking research focus (as Tamil Nadu is very close to Sumatra, approximately 2000 km).

This research is highly statistical and has been designed to address these gaps by studying the impacts of all major phenomena including ENSO, IOD and SST on NEMR pattern in TN. Thus, the goal of present research is to address the key issues related with temporal and spatial variability of rainfall patterns observed over the TN from 1982 to 2005 during the NEMR period and understand the possibility of any teleconnection relationship between 2004 earthquake and the recent rainfall fluctuations in TN.

### **1.3 Research Questions**

The goals of this research are to:

1. Identify the rainfall trend in Tamil Nadu to better understand its variability within the state.
2. Understand and determine the relation among the spatial and temporal variability of Tamil Nadu rainfall with respect to other phenomena, namely, SST, ENSO and IOD.
3. Evaluate the relationship between SST variability in 2004 Earthquake Epicenter region and Tamil Nadu rainfall during NEMR period.

## **1.4 Research Goals**

In order to achieve the research questions, this research attempts to address the following research goals with respect to Tamil Nadu rainfall and its relationship with other phenomena.

### **Tamil Nadu Rainfall**

1. Is the rainfall pattern uniform across the state of Tamil Nadu suggesting spatial variation?
2. Does Tamil Nadu's rainfall pattern vary within a year implying the presence of temporal variation?

### **Relationship with other phenomena**

3. Does spatial variation of other phenomena, namely, SST, ENSO and IOD have any influence over Tamil Nadu's rainfall?
4. Does temporal variation of other phenomena mentioned above affect Tamil Nadu's rainfall?
5. Importantly, do rainfall values change with changing SST values? In addition, does an earthquake event result in high rainfall values to near-by areas?

## 1.5 Hypotheses

### Tamil Nadu Rainfall

#### **Hypothesis 1: The rainfall pattern is not uniform across the state of Tamil Nadu.**

Rainfall values similar to other global phenomena are dependent on the topography, spatial location and other natural factors surrounding the place. Further, Tamil Nadu is in the south-eastern peninsular part of India surrounded by waters on its eastern and southern regions. This greatly affects the rainfall patterns in the southern, eastern, northern and western regions of the state. This will be tested by considering different rainfall domains within the state to evaluate the rainfall variations (or non-variations) in the state.

#### **Hypothesis 2: Tamil Nadu's rainfall pattern varies even with time.**

As mentioned earlier, India receives both SWMR and NEMR and Tamil Nadu receives half of its rainfall during NEMR period. Despite the huge contribution of NEMR in Tamil Nadu, certain western parts of the state receive high rainfall during the summer monsoon owing to its proximity to the Western Ghats of India. This will be tested by considering the monthly rainfall variations for the above mentioned rainfall domains. This would help in comprehending any variations (or non-variations) present over different time periods.

**Hypothesis 3: The global phenomena such as SST, ENSO, and IOD, affect rainfall pattern in Tamil Nadu.**

The close proximity of Tamil Nadu to Indian Ocean results in a significant influence of oscillation indices and SST over its rainfall. Also, the vastness of Pacific Ocean results in an impact of the southern oscillation over global monsoon pattern. This will be tested by considering different SST regions (or Nino regions) over the Pacific and Indian ocean to evaluate the impact/change in rainfall due to these different regions considered.

**Hypothesis 4: The variations of these global phenomena over the period of time, i.e. starting from January to December in a year, greatly influence the rainfall pattern in Tamil Nadu over changing time period.**

Not only does the spatial variation control Tamil Nadu' rainfall pattern but also the temporal variation of these global phenomena affect it the most. This could be seen in the variation of rainfall values within the NEMR period, implying different factors occurring over different time periods influence rainfall pattern differently. This will be evaluated by performing a time-lag correlation analysis between the different SST regions considered and rainfall over Tamil Nadu.

**Hypothesis 5: Rainfall values are positively correlated with SST values.**

As SST values increase, the sea surface is warmed up resulting in evaporation of the surface water. This leads to the formation of moisture-laden clouds over the surface which moves along the wind direction and precipitate over adjacent areas of high sea surface temperatures.

**Earthquake event, like that of 2004 event in Sumatran region, results in high rainfall values in nearby areas of the event.**

Earthquakes events have a couple of precursors that significantly increase prior to an event. Surface Latent Heat Flux (SLHF) and SST are known to increase few days before an event because of the building stress and energy within the surface. This leads to evaporation of surface water followed by formation of moisture-laden clouds that eventually result in precipitation. I, therefore, hypothesize that such increasing values of SLHF and SST would result in increasing rainfall values to nearby places depending on the wind direction. This will be evaluated by performing a Principal Component Analysis which would help obtain the main factors that explain the most variance in rainfall over Tamil Nadu.

## **1.6 Research Need**

Tamil Nadu has been witnessing varying rainfall values in the past few years which are very well evident in the images shown below (Figure 1.2 and 1.3). The following pictures taken during NEMR period (November in particular) clearly reveal rainfall variability in Chennai. While the monthly average rainfall during the month of November for Chennai is around 300 mm (Indian Meteorological Department, Chennai), it poured almost 215 mm within 24 hours in November 2005; whereas, after two years i.e. in November 2007, barely a monthly average of 95 mm was recorded in Chennai. Again in a year's time, in 2008, 556 mm of rainfall was recorded for the month of November for Chennai (Image Sources: [www.anothersubcontinent.com](http://www.anothersubcontinent.com), [www.indiatimes.com](http://www.indiatimes.com), [www.thehindu.com](http://www.thehindu.com)).



(a)



(b)

*Figure 1.2: November 2005 Rainfall in Chennai (recorded value: 215mm in 24 hours); (a) & (b) illustrate the damage and costs brought about by 2005' aggressive rainfall*



(a)



(b)

*Figure 1.3: November 2008 Rainfall in Chennai (recorded value of monthly rainfall: 556 mm); (a) & (b) illustrate flooding occurrence in the residential areas of Chennai metropolitan area caused by 2008' downpour.*

This variation in rainfall is clearly depicted from the following precipitation anomaly graph which shows a combination of dry and wet years during this monsoon season (i.e. values are graphed for the months of ‘October’, ‘November’ and ‘December’ for each year starting 1990 to 2008). This variability has affected the local economy and agricultural practices in a drastic manner that study of rainfall variability is of utmost concern to help improve the water management practices in Tamil Nadu (Geethalakshmi et. al, 2003).

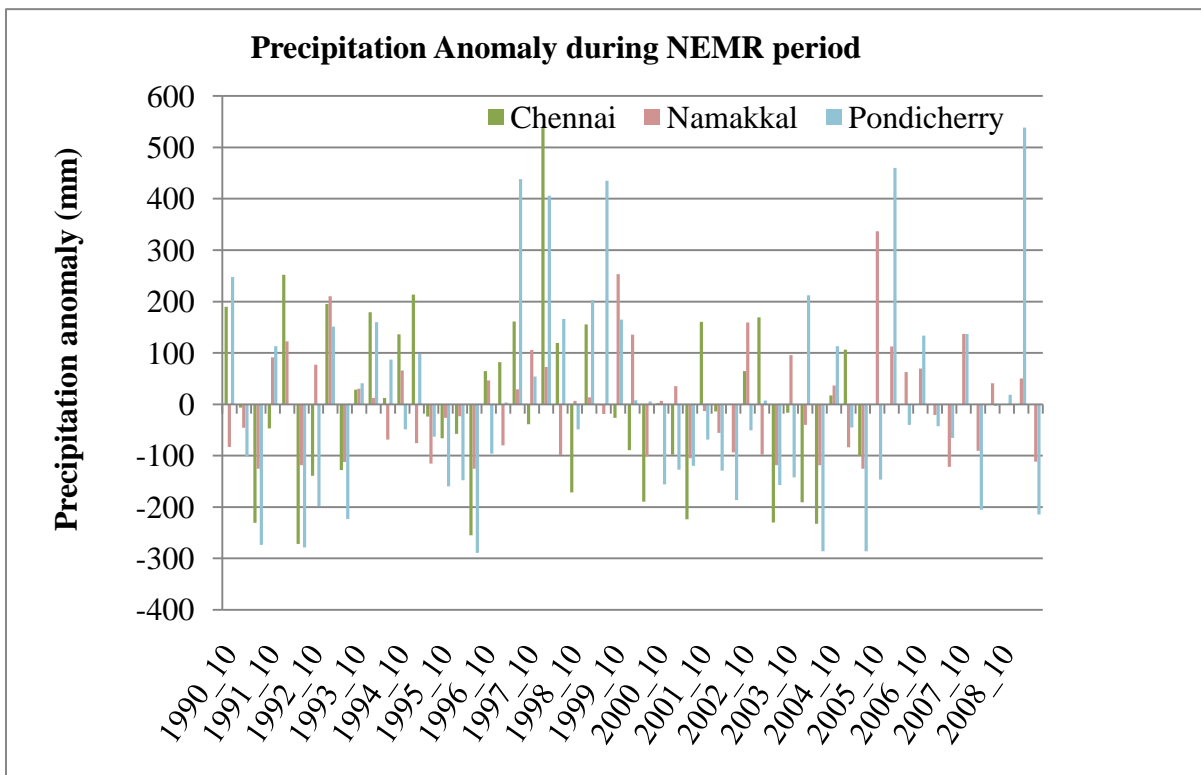


Figure 1.4: Precipitation Anomaly during NEMR period for the cities of Chennai, Namakkal and Pondicherry with a main focus on the recent decades (1990 – 2008).

Mean precipitation during NEMR period - Chennai:273 mm; Pondicherry:298 mm;

Namakkal:125 mm

Precipitation anomaly was calculated by deducting mean precipitation value observed over a period of 1990 to 2008 for Namakkal and Pondicherry, and 1990 to 2004 for Chennai (values given above) during NEMR period from each observed value (i.e. climatology deduction) of these 3 stations. It reveals rainfall variability observed in these places. Thus, there is a great need for a thorough understanding of rainfall variability in the South-Eastern state of India, Tamil Nadu.

Moreover, Tamil Nadu' NEMR variability lacks a rich literature of documentation as mentioned earlier. This is stated with the evidence of wrong assignment of geographical boundaries for SST regions used by Geethalakshmi et. al., (2009). In this research study, Saji-East' and Saji-West' geographical locations have been interchanged in Table I (used in the article), and these were maintained throughout the article for discussing the results. Thus, correlation matrix results obtained from this article are not reliable. This along with lack of literature doubly necessitates a comprehensive study of the NEMR variability in Tamil Nadu.

## **1.7 Research Relevance**

The long term goal of this research study is to provide inputs to studies involving moisture transport and climate modeling for South India which would require a comprehensive knowledge of the rainfall pattern in TN. Furthermore, the completion of this research would be vital in the investigation of the debatable earthquake prone zone which would help confirm the significance of SST variations in this region over rainfall distribution in TN. This underscores the uniqueness and innovativeness of this project. Finally, this study proposes a novel phenomenon— tectonoprecipitation— whereby precipitation is influenced by the heat released by seismic events.

## CHAPTER 2

### LITERATURE REVIEW

#### 2.1 Monsoon Forecast – An Overview

Rainfall patterns and their variability throughout the globe is a much studied research topic, and various indices affecting these patterns are being analyzed. The first ever monsoon forecast was performed by H.F. Blanford (1884), which marked the official start of monsoon forecasting as early as 1880s. Followed by this start were Hildebrandsson (1897)'s discovery of pressure opposition between Sydney and Buenos Aires, Lockyers and Lockyers (1902)'s confirmation of the see-saw between pressure around Indian Ocean and Argentina and a system of pressure classification based on this oscillation (Normand, 1953). Sir Gilbert Walker (1923, 1924) had a breakthrough of discovering three large scale see-saws: the North Atlantic, North Pacific and Southern Oscillations (SO) (Walker, 1925). The northern oscillations were regional phenomena while the Southern oscillation had a global effect. The oscillations (with irregular periodicity) discovered by Walker were stated by Normand (1953) as “...*They are related to but not controlled by sunspots, and they are to be regarded, in Walker's words, 'as a systematic swaying of inter-connected world conditions, which is intensified or checked by solar changes.'* ”. ‘Southern Oscillation’, a term coined by Sir Walker described a set of climatological relationships between Indian and Pacific Ocean regions which was, later famously, referred as Walker circulation. This circulation was described as the zonal component and the classical Hadley cell as the meridional component (integrated over all latitudes) of a quasi-stationary ultralong wave system tied to land-sea distribution by Flohn, H. (Pant and Parthasarathy, 1981). Wright came up with a long time series of the southern oscillation index (SOI) for the period

1851 – 1974, which was based on the pressure values and weighted average of the mean sea level pressure values. The behavior of SOI as defined by him, “*some times the circulation is stronger than usual (high index) and then it is associated with increased upwelling of cold water, clear skies and low rainfall in the equatorial Pacific, and relatively cloudy rainy conditions in Indonesia, east Australia and India. At other times the Walker cell is weaker than usual (low index) and then the oceanic upwelling is also weak, associated with conditions in the Indian Ocean sector. The fluctuation between these states is the southern oscillation.*” (Pant and Parthasarathy, 1981). This discovery was later followed by a flurry of research works on monsoon variations and its relation to the SO and to SST. Thus, the forecast study of the Indian monsoon led to an examination of world-wide variations of weather, with an initial research interest on sunspots and pressure, temperature and rainfall over the world (Norman, 1953).

## **2.2 ENSO**

### **2.2.1 ENSO and SOI – An Overview**

ENSO is a quasi-periodic phenomenon occurring in an irregular period ranging from three to five years (Pant and Parthasarathy, 1981), It is an ocean-atmospheric-coupled phenomenon that occurs across the tropical Pacific Ocean. Two phases, namely, El-Niño and La-Niña have been recognized. El-Niño refers to the extensive warming of the central and eastern Pacific that leads to a major shift in weather patterns across the Pacific. La Niña refers to the extensive cooling of the central and eastern Pacific Ocean.

The fluctuations in Equatorial-Pacific SST during El Niño and La Niña are accompanied by larger-scale air pressure fluctuations (i.e. the Southern Oscillation). The negative phase of the

Southern Oscillation occurs during El Niño episodes, when abnormally high air pressure covers the western tropical Pacific (i.e. near Indonesia) and abnormally low air pressure covers the eastern tropical Pacific (i.e. near western coast of South America). In contrast, the positive phase of the Southern Oscillation occurs during La Niña episodes, when abnormally low air pressure covers western tropical Pacific and abnormally high air pressure covers eastern tropical Pacific (Rasmusson and Carpenter, 1982).

SOI, a measure of the pressure anomaly between the eastern and the western Pacific, is calculated from the monthly or seasonal fluctuations in the air pressure difference between Tahiti (east of the dateline) and Darwin (west of the dateline) or the standardized anomaly between the Mean Sea Level Pressure between Tahiti and Darwin.

$$SOI = \frac{10[P_{diff} - P_{diffav}]}{SD(P_{diff})}$$

Where,

$P_{diff}$  = (average Tahiti MSLP for the month) - (average Darwin MSLP for the month),

$P_{diffav}$  = long term average of  $P_{diff}$  for the month in question, and

$SD(P_{diff})$  = long term standard deviation of  $P_{diff}$  for the month in question.

(Source: Australian Bureau of Meteorology)

Discovery of the Walker circulation was soon followed by a number of analyses indicating a link between the SO and El-Niño (Berlage 1966; Bjerknes 1966, 1969, 1972; Kidson 1975). Later on, studies relating SO variations in SST over the tropical Pacific (Rasmusson and Carpenter, 1982), correlating rainfall anomalies and ENSO around the globe (Ropelewski and Halpert's 1987, 1989), establishing a correlation between annual rain anomaly with bimonthly average SST

anomaly over the equatorial Pacific (Dai et al., 1997), and confirming ENSO to be the major driver of the interannual variability of global rainfall (Haddad et al., 2004) were conducted.

### **2.2.2 Niño Regions and SST**

Under normal conditions, winds blow from 30 °S and 30 °N towards Equator that under the Coriolis effect (an apparent deflection of moving objects or an inertial force described by Gustave-Gaspard Coriolis in 1835) curves towards west. This effect results in easterlies (i.e. wind blowing from east to west) that cause an accumulation of sea water in the western region resulting in an increase in SST. This phenomenon leads to rising warm air forming clouds and results in an increase in rainfall for that part of the globe where SST is higher than normal. Thus, SST plays an important role in rainfall variability. When the easterlies diminish, the warm surface water shifts eastward and an ENSO cycle starts.

Different techniques have been used to define El Niño/La Niña events. The most common ones are the SOI and the Niño regions. The Niño regions (Figure 2.1; Table 2.1) refer to the SST anomalies in defined parts of the Tropical Pacific Ocean. Literatures describe five regions of interest for ENSO event in the Pacific: Niño-1+2 consisting of Niño-1 and Niño-2, Niño-3, Niño-4, and Niño-3.4. ENSO event is determined by computing 5-month running mean of SST anomalies in these Niño regions, which is then used to smooth out the possible seasonal variability in the tropical ocean.

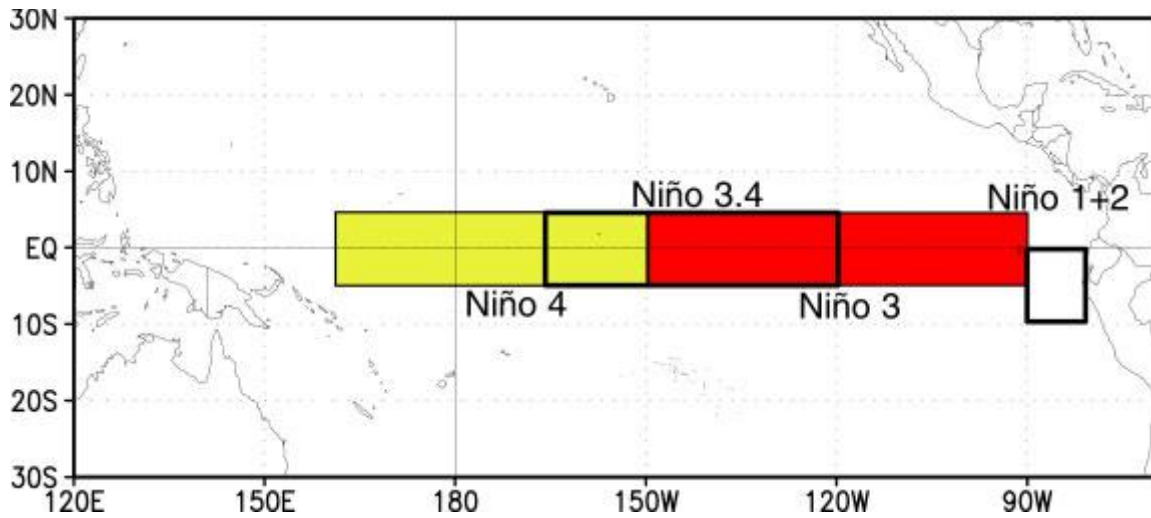


Figure 2.1 Niño Regions (source: [www.cpc.noaa.gov](http://www.cpc.noaa.gov))

Table 2.1 Niño Regions

NINO REGIONS	LATITUDE	LONGITUDE
Niño-1+2	0° - 10°S	90°W - 80°W
Niño-3	5°N - 5°S	150°W - 90°W
Niño-4	5°N - 5°S	160°E - 150°W
Niño-3.4	5°N - 5°S	170°W - 120°W

An SST anomaly of  $+0.5^{\circ}\text{C}$  ( $-0.5^{\circ}\text{C}$ ), defines El Niño (La Niña) phase in Niño-3 region, and the SST anomaly should exceed  $+0.4^{\circ}\text{C}$  ( $-0.4^{\circ}\text{C}$ ) for an El Niño (La Niña) in Niño-3.4 region (Source: [www.orca.rsmas.miami.edu](http://www.orca.rsmas.miami.edu)).

Although studies concentrating on the influence of Niño regions' SST over NEMR in South India (or Tamil Nadu in particular) are gaining their importance, not many have been undertaken a research to fully understand this relationship (Kumar et al., 2004; Revadekar and Kulkarni,

2008). It was observed that Niño 3.4 regions' SSTs and SOI are positively and negatively correlated respectively with NEMR and work well in assessing NEMR over coastal Andhra Pradesh (Kumar et al., 2004). High correlation between April SSTs over the Niño 3.4 region and the frequency and intensity of extreme precipitation events in South East India was analyzed. Relationships between extreme rainfall events and ENSO need to be examined thoroughly to understand the mechanism of such precipitation events (Revadekar and Kulkarni, 2008).

A more specific study of a NEMR-ENSO relationship for Tamil Nadu was carried out to confirm the significant influence of SO and El Niño-3 SST on NEMR. This was demonstrated using a composite circulation analysis which showed that an increase in NEMR in Tamil Nadu during El-Niño years was because of positive sea level pressure (SLP) anomalies over the Bay of Bengal and negative SLP anomalies over the Arabian Sea resulting in strong north-easterly winds. The analysis also presented weaker statistical relationships between the Indian Ocean Dipole mode and NEMR than ENSO and NEMR (Geethalakshmi et al., 2009).

Although, a great amount of time and work have been dedicated to the relationship between the Indian monsoon and ENSO/SST, South India (in specific, Tamil Nadu)'s NEMR relationship with ENSO and SST need to be more clearly understood for a complete mechanism update. This is due to the fact that SWMR and NEMR are not influenced by ENSO in the same way; they are negatively and positively correlated, respectively, with negative SST anomalies (as seen from the above mentioned literatures).

### 2.2.3 ENSO and Indian Monsoon

Several studies have examined the correlation between the Southern Oscillation Index (SOI) and the Indian summer monsoon rains from June through September (Sikka, 1980; Rasmusson and Carpenter, 1983; Shukla and Paolina, 1983; Parthasarathy and Pant, 1985; Kumar et al., 1999) indicating a decrease in monsoon rainfall as the Darwin pressure anomaly decreases below normal. It was observed that SWMR was influenced by planetary scale features such as the Hadley Circulation and Walker Circulation, which depend on the variations of meridional and zonal temperature gradients respectively (Sikka, 1980). Further, warm episodes in the eastern-central Pacific Ocean (i.e. high SST in the eastern and low SST in the western Pacific Ocean) were found to be influencing SWMR resulting in catastrophic droughts in India. In addition, it was noted that major droughts have occurred in other non-warm episode years too; implying a detailed investigation of warm episode circulation anomalies over Indian region was certainly required (Rasmusson and Carpenter, 1983). The tendency of the Darwin pressure anomaly before the SWMR period was considered a good indicator of the monsoon rainfall anomaly, in which it was used to demonstrate the non-occurrence of droughts and heavy rainfall in India. Using this relationship, Shukla and Paolini illustrated that the warm SST anomalies in the equatorial Pacific and fluctuations of monsoon rainfall were two important forcing functions for atmospheric circulation anomalies (Shukla and Paolini, 1983). In contrast, South India displays an opposite trend: It tends to have wet anomalies during El-Niño (SOI negative) years (as cited by Geethalakshmi et al., 2009; Singh and Chattopadhyay, 1998; Jayanthi and Govindachari, 1999; Khole and De, 2003).

While some studies (Kumar et al., 1999) suggesting the recent weakening of relationship between ENSO and SWMR, other studies concentrate on ENSO's strengthening relationship

with NEMR. A shift in the mean position of the Walker circulation anomalies and increased land-sea gradients were attributed for the former weakening relationship; however, no such large shifts were observed for the correlation between NEMR and ENSO. It has been suggested that unlike its counterpart, NEMR's correlation with ENSO has been on a remarkable rise for peninsular India. It was also found that SSTs over the central and western IO have been increasing in recent decades and this trend is likely to modulate both the monsoon circulation and ENSO's influence resulting in enhanced rainfall during El Niño episodes in NEMR period (Zubair and Ropelewski, 2006). This was supported by a study on the secular variations on the relationships between NEMR over South Asia and ENSO, in which it was stated that above-normal NEMR was experienced due to stronger easterly wind anomalies and anomalous low-level moisture convergence in the circulation regime over southern India and Sri Lanka (Kumar et al., 2007).

## **2.3 IOD**

### **2.3.1 IOD and DMI – An Overview**

The Indian Ocean borders Australia, Indonesia, Africa and the southern part of India. As a result these countries are often referred to as Indian Ocean rim countries. Normally, the Indian Ocean is warm in the east and cool in the west, and this temperature is associated with westerly winds (originating from the west and moving towards the east) blowing towards Indonesia (Kripalini and Kumar 2004). However, recent research by Saji et al., (1999) and Webster et al., (1999) has discovered a dipole mode, referred to as the Indian Ocean Dipole (IOD), in the tropical Indian Ocean region, similar to the El-Niño Southern Oscillation (ENSO) in the Pacific Ocean. Further, these studies have confirmed the presence of strong ocean-atmosphere-land interactions in the

Indian Ocean that are self-maintaining. IOD is an irregular oscillation of Sea Surface Temperatures (SST) in the Indian Ocean. The ocean dynamics that are a result of an IOD event, wind anomalies, Rossby waves structure and strong ocean-atmosphere interactions lead to irregular oscillations of SSTs resulting in a dipole mode. Scientists are still working on understanding the phenomenon completely and its causative factors.

There are two main phases related to the IOD mode which are called “Positive Event” (Figure 2.2 (a)) and “Negative Event” (Figure 2.2 (b)). During a positive IOD event, the western region of the Indian Ocean has anomalously warm temperatures and eastern region has anomalously cool SST, which is reversed for a negative event. The event is characterized by seasonal phase locking: a phase when significant SST anomalies appear around June, intensify in the following months and peak in October. Further, a tight coupling between zonal wind anomaly and dipole intensity is observed which results in a tendency for a dipole mode event to be preceded by an opposite polarity event (biennial tendency, in other words, positive and negative events have a tendency to alternate) (Saji et al., 1999). This mode induces unusual rainfall distributions along the Indian Ocean rim countries (Kripalini and Kumar 2004). This dipole mode has been observed to account for 12% of the SST variability in the Indian Ocean and the rainfall variability in eastern Africa and droughts in Indonesia during its active years (Saji et. al., 1999). Therefore, a clear understanding of SST variations caused by IOD event would help achieve a better understanding of rainfall variations in these countries.

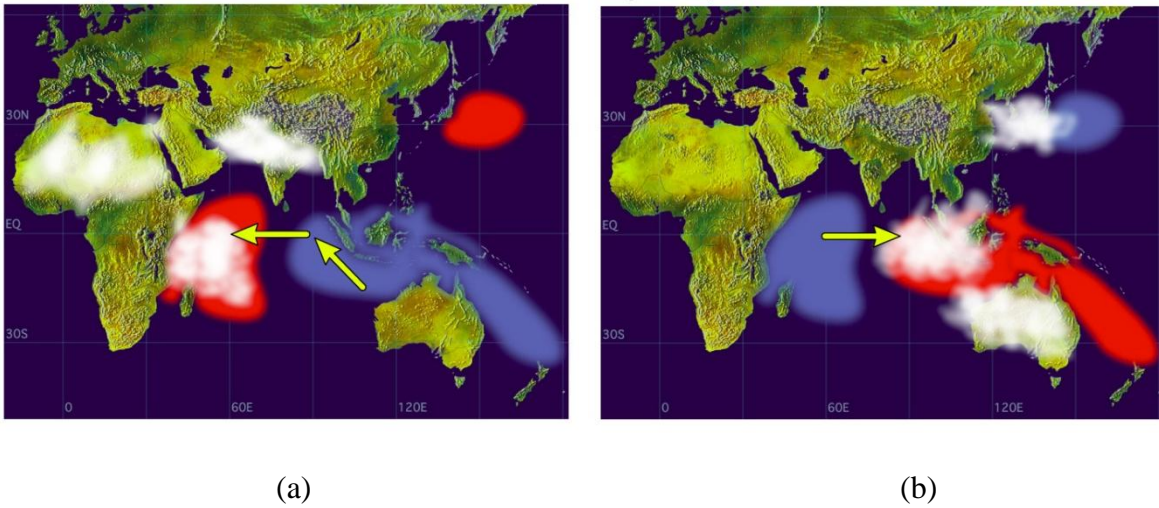


*Figure 2.2 Dipole Events (a) Positive Dipole Event (b) Negative Dipole Event*

SST anomalies are shaded in the images given above (red color is for warm anomalies and blue is for cold anomalies). White patches indicate increased convective activities and arrows indicate anomalous wind directions during IOD events.

Source: <http://www.thenakedscientists.com/forum/index.php?topic=20469.0>

An IOD event is identified using an index proposed by Saji et al. (1999), the DMI (Dipole Mode Index), which is the difference in SST anomalies in the western ( $50 - 70^{\circ}\text{E}$ ,  $10^{\circ}\text{S} - 10^{\circ}\text{N}$ ) and south eastern ( $90 - 110^{\circ}\text{E}$ ,  $10^{\circ}\text{S} - \text{Equator}$ ) regions of IO. These regions are termed as Saji's West and Saji's East boxes respectively. These regions are selected based on the characteristic SST anomaly reversal and through an Empirical Orthogonal Analysis (EOF; Saji et al., 1999). In other words, positive and negative IOD events result in changing SST anomalies in the western and eastern regions of Indian Ocean. Extreme IOD events are identified as years during which annual mean of DMI exceeds one standard deviation of normalized index and SST values (Rao et al., 2002).

### 2.3.2 ENSO & IOD Interactions

With the discovery of IOD coupled phenomena in IO region, several studies (Allan et al., 2001; Hastenrath, 2002; Baquero et al., 2002) have interrogated the independence of an IOD event and its possible relation, if any, to ENSO. With coupled ocean-atmosphere general circulation models (CGCM), results have been analyzed to prove that ocean dynamics were not important for IOD-like SST variability and that IODs are primarily associated with ENSO variability. Further, an ENSO-independent oscillatory mode was quite not evident in CGCM studies, which disproved the earlier description of a homogenous response in IO with respect to ENSO's variability. It was concluded that a dipole-like SST variability existed that was forced by surface heat flux anomalies and also driven by coupled ocean-atmosphere interactions (Baquero et al., 2002). Other studies confirmed the existence of a proper mechanism for a dipole evolution in IO similar to ENSO in Pacific Ocean with their simulation of the dipole mode events using CGCMs (Behera et al., 2000; Iizuka et al., 2000; Vinayachandran et al., 2002). Behera's study of SST variability in the tropical IO using an intermediate 2.5-layer ocean model revealed the influence of interannual heat fluxes – primarily latent heat flux and radiative flux – over SST anomalies. Iizuka's heat budget analysis demonstrated an air-sea interaction, influenced by ocean dynamics, was essential for this evolution. Also, Vinayachandran's ocean model study of heat budget confirmed that the cooling of the eastern IO during positive IODs was caused by upwelling, while the subsequent warming was caused by surface heat flux.

A study of interannual variability in subsurface tropical IO has revealed IOD's influence over the region leading to an interesting discovery of ENSO-IOD interaction in this region. In this part of the region, SST variability is governed by ENSO, while the subsurface variability is dominated by the IOD that is controlled in turn by equatorial zonal winds (Rao et al., 2002). A noENSO

experiment was conducted using a CGCM in order to examine the independent evolution of IOD by decoupling tropical Pacific Ocean from atmosphere, and was found to be in consistent with other previous statistical results obtained by linearly separating ENSO effect from observed data (Yamagata et al., 2003; Behera et al., 2003) in demonstrating the independence existence and dominance of IOD during nonENSO years. In addition, IOD's periodicity, strength, and formation processes were affected by ENSO variability in years of co-occurrences (Behera et al., 2006).

### **2.3.2 IOD and Indian Monsoon**

The IOD influences the correlation between ENSO and SWMR such that a high IOD-SWMR correlation leads to a low ENSO-SWMR correlation (needs a citation). ENSO-induced anomalous circulation over Indian region has either been countered or supported by the IOD-induced circulation based on the phase and magnitude of the ocean-atmosphere-coupled phenomena (Ashok et al., 2001).

The decadal variability of IOD reveals negative phase dominance from 1880 – 1920 and positive phase dominance from 1960 – 2000 with a suppressed activity in between the two periods. Further, NEMR variability in South India is enhanced during the positive phase of IOD and suppressed during the negative phase of IOD. This occurs due to the diverging (converging) wind pattern from (towards) southern parts of India and converging and transporting moisture towards Sumatra (South India) during a negative (positive) phase (Kripalini and Kumar 2004).

However, there are differences in opinions about the mechanisms or factors responsible for NEMR variability in South India, Tamil Nadu specifically. One school advocates that SST variability and IOD are dominated by ENSO (Allan et al., 2001; Baquero et al., 2002; Annamalai et al., 2003; Vaid et al., 2007) and the other promotes IOD as an event independent of ENSO (Behera et al., 2000; Iizuka et al., 2000; Vinayachandran et al., 2002) which seems to be the main factor in monsoon variability in Tamil Nadu in addition to SST anomaly in IO. Thus, the question of which factor plays a major role in monsoon variability needs to be completely understood. The present study addresses these questions.

To be more specific, this study explores the role of ENSO, IOD, and SST regions in Pacific Ocean and Indian Ocean regarding NEMR variability both separately and together to find out the magnitude of impact from each factor as well as all of them together. Further, it investigates the efficiency of SST monitoring in the above said regions for NEMR variability check and monitoring. From, the previous studies (Ashok et al., 2001; Rao et al., 2002; Geethalakshmi 2009), it is evident that the contribution of ENSO alone cannot explain the monsoon variability completely. The role of ENSO, IOD and SST are therefore examined using regression model and EOF analysis.

## **2.4 Sumatra-Andaman Earthquake – An Overview**

### **2.4.1. Slip Process**

The 26 December 2004 Sumatra-Andaman earthquake (Moment magnitude – 9.1 to 9.3) was one of the largest earthquakes in more than 40 years and it produced a devastating impact on the Indian Ocean region of the world. Not only did it result in a megathrust rupture but also it

produced huge Tsunami waves of about 30 – 50 m along the western Aceh coast. The impact was most severe in the largest city of the Indonesian region - Banda Aceh, where more than 100,000 people were killed (Shearer and Burgmann, 2010).

The epicenter of this earthquake event was near the junction of three major tectonic plates, namely, Indian plate, Eurasian plate and the Australian plate. This region is thus a diffuse zone of seismicity and deformation, characterized by extensive faulting and numerous earthquakes. Similar to previous earthquakes that occurred further North, in the Andaman Sea and further South along the Sumatra, Java and Sunda sections, this earthquake event also occurred along one of the earth's greatest fault zones, a subduction zone (one in which a tectonic plate moves under another tectonic plate sinking into the Earth's mantle, as the plates converge) known as the Sunda Trench. This trench extends all the way from the eastern Himalayas and trends southward through Myanmar, continuing past Sumatra and Java and far East towards Australia and the lesser Sunda Islands ending up near Timor (Lay et. al, 2005).

Rupture front travels up the fault to about 14°N. Short period energy radiated shows strong directivity, ~500 s duration  
 $V_r \sim 2.5 \text{ km/s}$

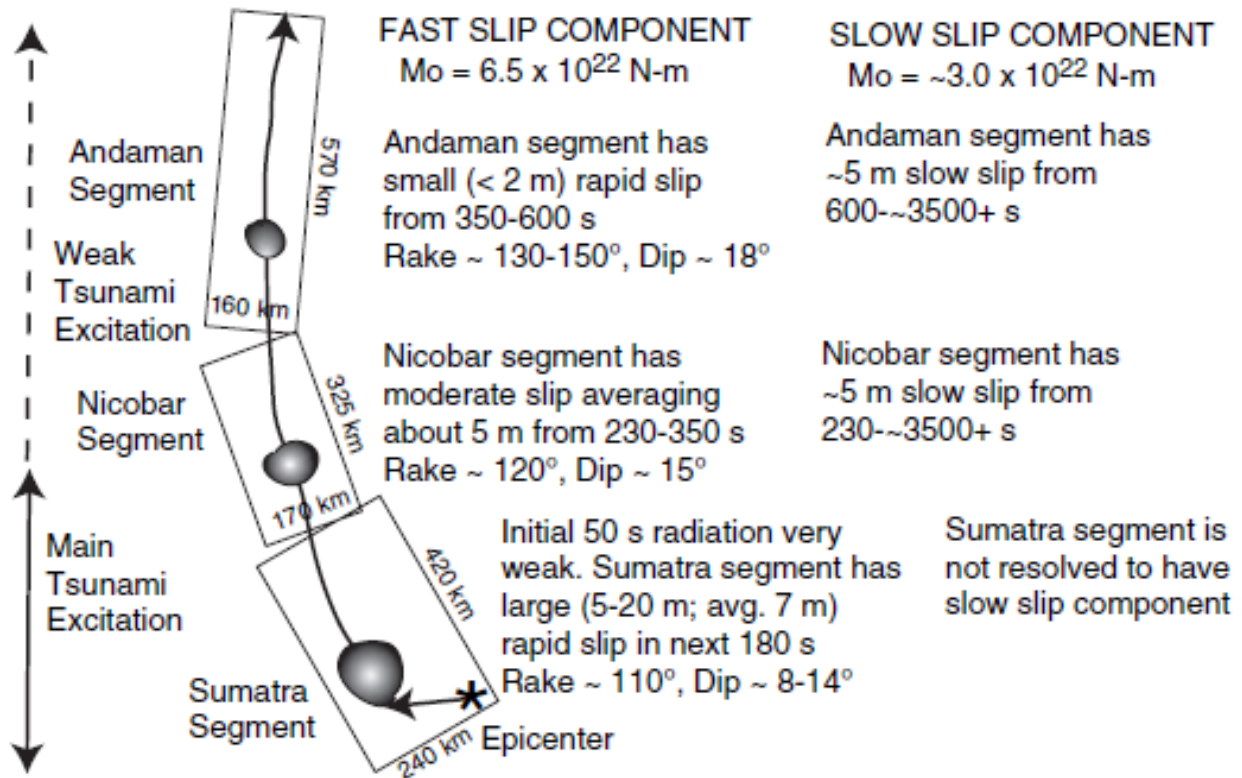


Figure 2.3 Sub-division of the earthquake rupture zone into Sumatra segment, Nicobar segment and Andaman segment (Lay et. al., 2005)

It is observed that the Indo-Australian plate moves generally northward at 40 to 50 mm/year and the 2004 earthquake ruptured the boundary between the Indo-Australian plate and the southeastern portion of the Eurasian plate (segmented into Burma and Sunda subplates). The longest known earthquake rupture was observed by this earthquake. This is explained well by Lay et. al, 2005, which is also re-produced here. For the purpose of explanation, Lay et. al, 2005 have subdivided the rupture zones into three segments, namely, Sumatra segment, Nicobar segment and the Andaman segment, according to the inferred rupture process. As illustrated in

Figure 2.4, the rupture began at the southeastern edge of the Sumatra segment and propagated to about 1200 km north of the epicenter with a rupture velocity of 2.0 to 3.0 km/s. This event generated most of the slip (or relative movement) in the southern half of the rupture zone that caused the seismic waves. It is observed that this event has been a compound process of seismic-energy release, involving variable slip amplitude, rupture velocities and slip duration. Additionally, the Andaman and Nicobar segments have small ( $< 2$  m) and moderate slips (5 m), as against the Sumatra segment with a large rapid slip (5 – 20 m). This has been a major strike-slip event (Lay et. al, 2005, Ammon et. al, 2005). Thus, this earthquake event was very complex process and requires more detailed analyses of the same.

#### **2.4.2. Precursors to an earthquake**

There have been a number of studies that were conducted analyzing important precursors that lead to an earthquake event. Among those, some of them have analyzed the 2004 Sumatran earthquake event and have identified anomalous changes in oceanic and atmospheric parameters. It has been found that Surface Latent Heat Flux (SLHF), Sea Surface Temperature (SST), water vapor (WV), cloud liquid water (CLW) increased anomalously a few days prior to the earthquake event (varying with each event) near the epicenter and decreased soon after the event and then recover to their normal value 5 days after the event (R.P. Singh et al., 2007; R.P. Singh et al., 2006; Meihua et al., 2006; Dey and R.P. Singh, 2003).

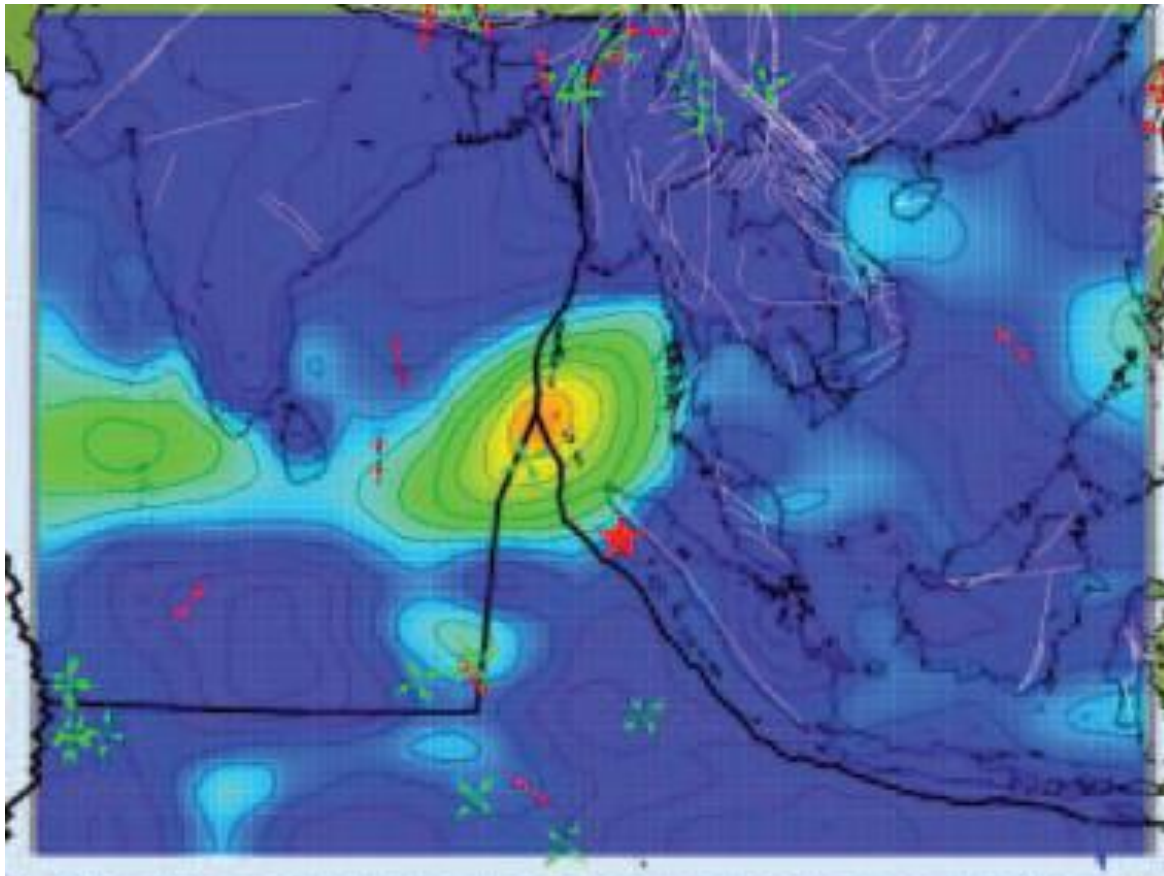


*Figure 2.4 Surface Latent Heat Anomaly – 07 December 2004 (Singh et al., 2007)*

It has been noted that SLHF is the heat released by phase changes due to solidification or evaporation or melting (Dey and R.P. Singh, 2003). It has been observed that infrared thermal (IR) temperature over the epicentral region prior to the earthquake increases that leads to an anomalous increase in SLHF before the event (Figure 2.4). This is explained as the accumulation of stress prior to the earthquake in the epicentral region which results in the increase in IR temperature. These changes are prominent in shallow focal depth earthquakes. Owing to the fact

that SLHF exhibits the exchange of water vapor in the atmosphere, an increase in water vapor is also observed along with these other changes. Thus, the accumulated stress has been examined to affect the energy exchange which in turn affects the above mentioned ocean-atmosphere parameters (Dey and R.P. Singh, 2003). As these studies have explained the change in SST values before an earthquake event over the epicentral region, this research study is interested in extending this argument to observe any possible relationship between SST and rainfall values over the areas closer to an earthquake epicenter. This would allow us to explain and understand the ocean-atmosphere phenomena better.

## CHAPTER 3

### STUDY REGIONS, DATA AND METHODOLOGY

#### 3.1 An Overview

The first section of this chapter elaborates in detail about the study regions (rainfall domains and SST regions) focused-on for this research study. This is followed by a detailed description of datasets used, their resolutions, spatial extents ...etc. Finally, the methodologies employed to analyze the dataset are explained.

##### 3.1.1 Tamil Nadu

Tamil Nadu, lying in the Southern Peninsular India, is completely sheltered by the Western Ghats (orographic barrier along the west coast of India) from the rain-bearing winds of the southwest monsoon (aka South West Monsoon Rainfall, SWMR). As mentioned earlier in the introduction, the retreat of southwest monsoon and the reversal of the pressure and wind distribution occur at the beginning of October. This results in a heavy downpour of north-east monsoon rainfall over this region of the country. During the northeast monsoon, the coastal (interior) parts receive about 60% (50%) of the annual rainfall (Rao Krishna and Jagannathan, 1953; Kripalini and Kumar, 2004).

As discussed earlier, Indian Ocean experiences a unique ocean-atmosphere coupling mode, named, Indian Ocean Dipole mode (IOD), which leads to anomalous warm SSTs over the western Indian ocean and anomalous cold SSTs in the eastern Indian ocean. The southern part of India is situated approximately near the center of this mode that peaks in the September –

November period while NEMR peaks in the October – December period i.e. both peak during boreal autumn with a lag of 1 month. Studies reveal positive correlation/relationship between NEMR over southern India and IOD (Kripalini and Kumar, 2004). Thus, this study, specifically, focuses on Tamil Nadu' rainfall variability and examines not only on Indian oceanic factors, but also on global factors such as ENSO and SST over Nino regions and Indian Ocean to better understand the impact of such global factors on NEMR in Tamil Nadu, in particular.

### **3.1.2 Sea Surface Temperature Regions**

In order study the impact of SST over NEMR, five main regions were chosen throughout the globe as shown in Figure 3.1. These regions are SST-1 (Saji-East region), SST-2 (Saji-West region), SST-3 (El-Nino 3 region), SST-4 (El-Nino 4 region) and SST-5 (2004 Earthquake Epicenter region).

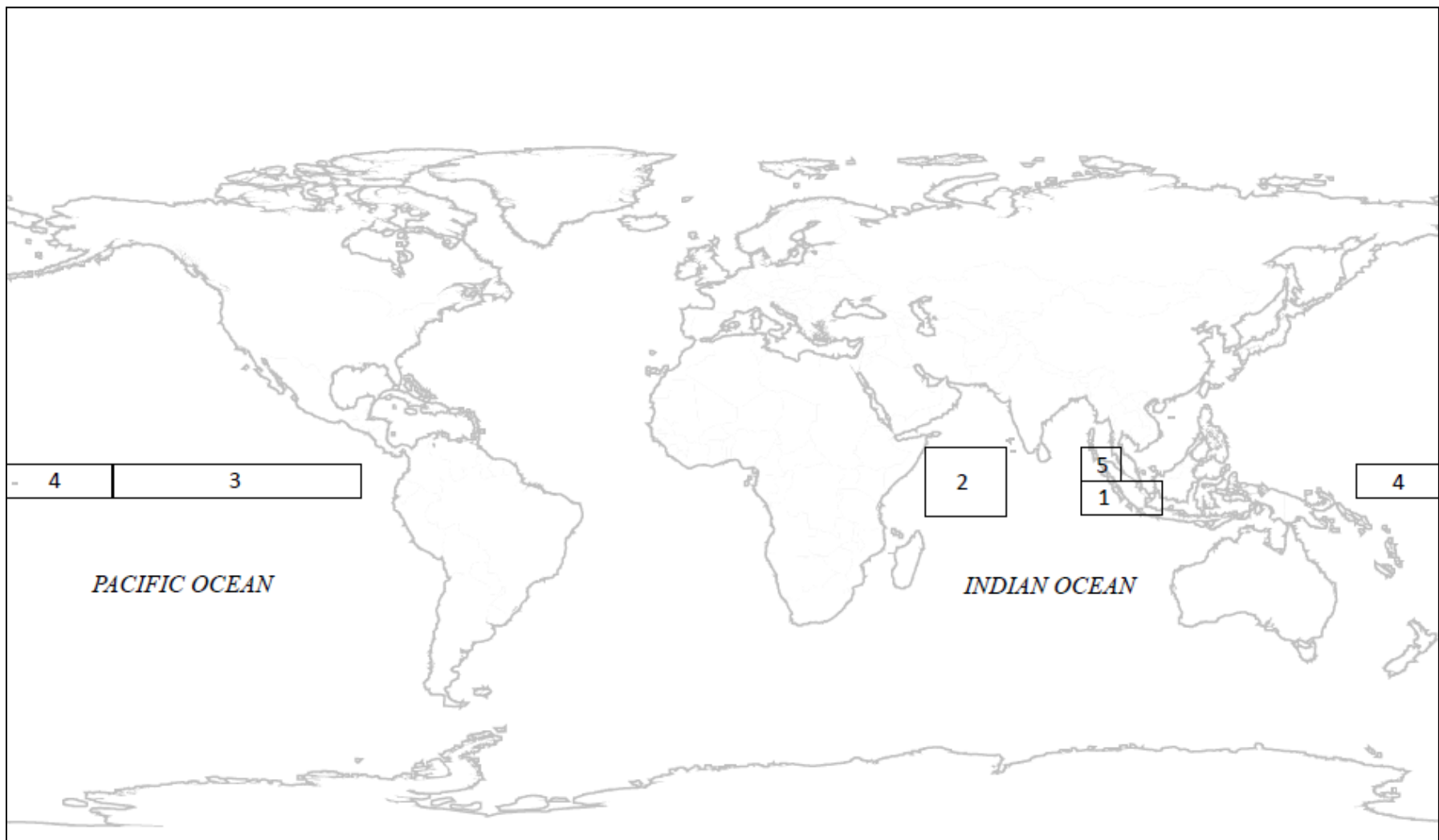


*Figure3.1: Sea Surface Temperature (SST) regions*

- 1: SST-1 (i.e. Saji East Region)
- 2: SST-2 (i.e. Saji West Region)
- 3: SST-3 (i.e. El-Nino 3 Region)
- 4: SST-4 (i.e. El-Nino 4 Region)
- 5: SST-5 (i.e. 2004 Earthquake Epicenter Region)

SST-1 and SST-2 are characteristic regions of the IOD. It has two events namely, positive and negative dipole events with significant SST changes observed in these regions. A positive event results in high SST values in SST-2 region and low SST values in SST-1 region while a negative event results in vice versa effect (Saji et al., 1999; Webster et al., 1999). Likewise, SST-3 and SST-4 are characteristic regions of the ENSO. It has two dipole events, namely, El-Nino and La-Nina with significant SST changes observed in these regions. El-Nino event results in high SST values in SST-3 region and low SST values in SST-4 region while La-Nina event results in vice versa effect (Bjerknes 1966, 1969; Kidson 1975). SST-5 is the region proposed in this research study to observe any SST change occurring in this epicentral region of 2004 Sumatran earthquake.

## **3.2 Datasets**

### **3.2.1 Rainfall**

Rainfall data used in this research study was purchased from National Climate Center, India Meteorological Department, Pune, India. The gridded dataset consists of daily rainfall values with a spatial resolution of 0.5 degree x 0.5 degree. It was developed using quality controlled

rainfall data from more than 6000 rain-gauge stations over India. These station rainfall values obtained for a period of 1971 to 2005 were interpolated into regular grids of 0.5 x 0.5 degree Latitude x Longitude using Shepard's method (1968; Rajeevan et. al., 2006). The interpolated dataset was also evaluated against another higher spatial resolution data obtained from a project named APHRODITE. Further information about the dataset can be obtained from the report titled 'A High Resolution Daily Gridded Rainfall Data Set (1971 – 2005) for Mesoscale Meteorological Studies' prepared by the National Climate Center, IMD, Pune.

The dataset obtained was in a gridded format (\*.grd) with rainfall values for each year in a separate file available for the entire country. This dataset was input into 'R' statistical software and an 'R' routine (R Program #1, Appendix A) was used to convert \*.grd files into R-readable arrays. This routine was also validated against the plots obtained from GrADS, Grid Analysis and Display System. Later, another program (R Program #2, Appendix A) was written to extract the rainfall values for the rainfall domains, explained in methodology section, in Tamil Nadu. The daily rainfall values were averaged into monthly means in order to be consistent with the other datasets used, as explained below.

### **3.2.2 Sea Surface Temperature**

Sea Surface Temperature file was freely distributed online by Earth System Research Laboratory, Physical Sciences Division. The product used in this research study was downloaded from <http://www.esrl.noaa.gov/psd/data/gridded/data.noaa.oisst.v2.html> on August, 27th, 2010. The NOAA Optimum Interpolation (OI) SST V2 product was obtained which was available for the global span of 89.5 degree N – 89.5 degree S, 0.5 degree E – 359.5 degree E with spatial

resolution of 1 degree Latitude x 1 degree longitude global grid (180 x 360). The SST values were monthly ones which were developed using a linear interpolation of the weekly values to daily values and then averaging the daily values to monthly. These files are currently updated since December, 1981. Along with the SST dataset, Land surface mask dataset (lsmask.nc) was also downloaded from the same website enabling the land pixels to be masked. Both these files were acquired in Netcdf format which were input into R and converted into arrays for specific SST regions using R Program #3.

### **3.2.3 Southern Oscillation Index**

Southern Oscillation Index, pressure anomaly difference between eastern and western Pacific Ocean (i.e. Tahiti and Darwin), was downloaded for the study period from National Weather Service, Climate Prediction Center (<http://www.cpc.ncep.noaa.gov/data/indices/>) on August, 27th, 2010. The dataset was available in an easy readable array format and the index values were obtained for each month starting 1982 to 2005.

### **3.2.4 Dipole Mode Index**

Dipole mode index measured as SST difference between western and eastern Indian Ocean (i.e. SST-2 and SST-1 regions) was downloaded from <http://www.jamstec.go.jp> on August, 27th, 2010. This monthly index was developed from HAdISST dataset for the period of 1958 – 2010. Similar to SOI, this was also available in an easy readable array format for individual months.

### **3.3 Methodology**

#### **3.3.1 Rainfall Domains**

As seen in Figure 1, Tamil Nadu is a South Eastern state of the Indian peninsular and is surrounded by Bay of Bengal to its east, Kerala, neighboring state, to its West and Indian Ocean to its South. Based on the 24-year monthly rainfall values, rainfall pattern is not uniform across the state. To identify similar regions of rainfall in TN, I further analyzed rainfall variation over space and time. First, annual rainfall variation for the entire state was calculated and graphed for each individual year in the study period, 1982 – 2005. This was executed using the ‘R’ statistical package (R Program #4, Appendix A) that plotted out rainfall variations for each individual year. Second, the range of rainfall values was estimated for each year to appreciate the dryness and wetness in each case. Finally, using these 24 years of data, the mean and range of rainfall value for the 24 year period were determined. Based on these values, four ranges of rainfall values were obtained considering the geographical area into account. Based on these rainfall values, four rainfall domains were selected. A one-way repeated measures ANOVA was used to compare the rainfall domains for statistical significant difference in their means. This resulted in the selection of two rainfall domains, namely, TN East and TN West, which will be explained in the next chapter.

#### **3.3.2 Time Series Analysis & Analysis of Variance**

The overall trend within each phenomenon can be understood from time series plots. These plots enabled a good comprehension of general behavior of each phenomenon and its cyclic or non-

cyclic/seasonal or non-seasonal pattern over the period of time. Although time series plots aided in a brief description about each phenomenon, the seasonal and cyclic effects inherent in the SST pattern did not lead to further analysis of the variance of the dataset. So, a one-way repeated measures ANalysis Of Variance (ANOVA), similar to the rainfall domains' variance analysis, was performed for SST regions and tested for significant differences. These differences were graphically represented using box-whisker plots (or 'box plots').

### **3.3.3 Time-lag Correlation**

Once, statistical significance was established among the study regions, time-lag correlation analysis was performed. Several atmospheric processes can act over long time periods; this analysis was designed to explore possible time-lagged relationships between TN rainfall and the periodic phenomena. This was conducted between the considered three factors (SST, DMI and SOI) and rainfall values for a particular domain in the study area. This technique is an extension of correlation analysis in which a time factor is considered for each correlation value i.e. the correlation between two variables over a period of time is estimated and the statistically significant difference over time is measured (Geethalakshmi et. al., 2009). Specifically this study is interested only in the NEMR period (October, November and December) rainfall values' correlation with January through December values of the other three factors. So, say, in TN East domain, correlation value between 24-year mean October rainfall and the other three factors is estimated for 12 months and this repeated for the other two months', namely, November and December, rainfall values. Hypothetically, if January SST-3 regions' SST value is positively correlated over November rainfall in TN East domain and is significantly higher than any other

months' SST value then, this would imply that a possible increase in SST value in SST-3 region during the earliest period of a year (i.e. January) could have high positive correlations over November rainfall for the study area. Thus, the SST change over this particular month could be paid more attention than other months with regards to the November rainfall. Although, correlation does not imply causal effect values, it is used as a major step in furthering the analyses and focusing on particular time periods/factors. Moreover, it helps identify the most and least correlated factors for the study area and period.

### **3.3.4 Principal Component Analysis and Regression model**

Principal Component Analysis (PCA) is an exploratory tool that was first proposed and designed by Karl Pearson (1901) to identify unknown trends in a multidimensional data set. This was further developed to its current modern form by Hotelling (1933) to be used in Psychology. Hence, it is also known as Hotelling's transform. Once the pattern is identified in the dataset, the original dataset is compressed or reduced in dimensionality without much information loss using orthogonal transformation. This allows further interpretation and exploration of the dataset (Hotelling H., 1933; Smith, L., 2002; Shlens, J., 2003; Garcia E., 2008).

This is explained as: *“It finds linear combinations of the original variables that are best linear predictors of the full set of variables. The principal components are derived as a sequence of orthogonal linear combinations of the dependent variable vector. Each linear combination has maximum capability to predict the full set of dependent variables subject to the condition that each combination is orthogonal to the previous linear combinations... Further, it is shown that the first  $r$  principal components have maximum capability to predict the dependent variable*

*vector among all sets of  $r$  linear combinations of the dependent variable vector ...”*  
(Christensen, 1991).

Given a set of correlated linear variables, PCA would enable transforming these variables into a set of uncorrelated (independent) variables called principal components, where the resulting variables are orthogonal to one another, i.e. each variable is perpendicular to the other irrespective of the number of dimensions. These orthogonally transformed and uncorrelated variables explain higher variance in the dataset than the original non-transformed and correlated variables. Hence, for the purpose of this study, after obtaining the correlations among the variables, PCA was adopted to narrow down the original correlated variables into a set of orthogonal variables which would explain the highest possible variance causing any influence over rainfall pattern in the study region. In order to accomplish the same, the following variables formed the original dataset for the study period: Consider a single rainfall domain, say, TN North, then input variables were SST values for SST-1, SST-2, SST-3, SST-4, SST-5, DMI, SOI and Rainfall values for TN North. PCA was then performed using SYSTAT, statistical software, which results set of eight eigenvalues and eigenvectors (the elements of eigenvectors are known as component loadings). The variables with the highest component loadings explain the greatest variance possible in the original dataset. In order to narrow down to variables explaining the highest variance, only those eigenvectors that had eigenvalues more than one (i.e. eigenvalue > 1) were considered and analyzed.

In total, these tools were used to test Hypotheses 1-5, and to identify relationships between TN rainfall and quasi-periodic phenomena over space and time. By understanding these relationships, we could then evaluate if it is even possible that thermal increases associated with Sumatran (or Javan) seismic activity could be teleconnected to rainfall in southern India.

Followed by PCA, the correlated variables were tested for their predictive nature using regression models. A step-wise regression analysis was performed in which backward elimination approach was followed. This process involves starting with all the candidate variables and testing them one by one for statistical significance, deleting any variable(s) that is/are not significant. At the end of this process, only those variables with good significance remain enabling the understanding of the predictive power of those variables in the model (Hocking R.R., 1976)

In this case, rainfall variability is considered as the dependent variable and all other variables (SST, DMI, SOI) are considered as independent variables which are tested for their significance in predicting TN's rainfall variability. This analysis would help understand those correlated and significant variables that have the most predictive power. Yet, these analyses do not help comprehend the causative/physical mechanism involved in the rainfall variability. This shortcoming is handled in limitations and conclusions sections of this document.

## CHAPTER 4

### RESULTS AND ANALYSIS

#### 4.1 Rainfall Domains in Tamil Nadu

The descriptive statistics (minimum, mean and maximum rainfall in a year) were calculated for each year of the 24-year study period for the state of Tamil Nadu (Table 4.1). As seen from the table, the average range (range is calculated as the maximum rainfall in a year minus the minimum rainfall in that specific year) for this study period was approximately 3649 mm per year with a minimum of 1620 mm per year and a maximum of 8136 mm per year. The outlier of maximum range happens to be in the year of 1984. Further, spatial distribution of annual rainfall over the study area was understood from the annual rainfall variation of the individual years. Moreover, in order to eliminate edge effect along the edges/boundaries of the state, few pixels have been included along the boundary, as can be seen from the western boundary of Tamil Nadu in these maps. For most of the years, except 1984 and 2005, western region has experienced maximum rainfall while the rest of the state has received either low or moderate rainfall. This spatial variation led to the calculation of a 24-year mean for the study area, as mapped in Figure 4.1. Based on these individual years and the 24-year mean rainfall distribution, the state was divided into four main domains, namely, “Purple Domain”, “Yellow Domain”, “Red Domain”, “Brown Domain” (the highlighted regions in Figure 4.2). Also, the rainfall range for these domains can be obtained from Table 4.2. This is depicted in the 24-year mean rainfall variation map.

*Table 4.1 Descriptive statistics of annual rainfall variation in Tamil Nadu for the 24 year study period*

<b>YEAR</b>	<b>MIN</b>	<b>MEAN</b>	<b>MAX</b>	<b>RANGE</b>
1982	368	866	2625	2257
1983	326	1133	4392	4066
1984	490	1175	8626	8136
1985	343	1045	3574	3231
1986	264	963	2617	2353
1987	282	1049	2572	2290
1988	371	1003	3053	2682
1989	74	930	2708	2634
1990	106	1046	3540	3434
1991	319	1314	4669	4351
1992	383	1236	4517	4133
1993	369	1254	3826	3457
1994	413	1201	3977	3564
1995	288	1096	3965	3677
1996	279	1243	4080	3801
1997	142	1220	4317	4176
1998	169	1289	5090	4922
1999	393	1180	4516	4123
2000	86	1150	4171	4085
2001	142	1092	4851	4709
2002	0	658	2986	2986
2003	0	641	3075	3075
2004	562	1481	4389	3827
2005	1482	2631	3104	1622

**24 year Mean Annual Rainfall Variations in South India,  
1982 - 2005 (mm per year)**

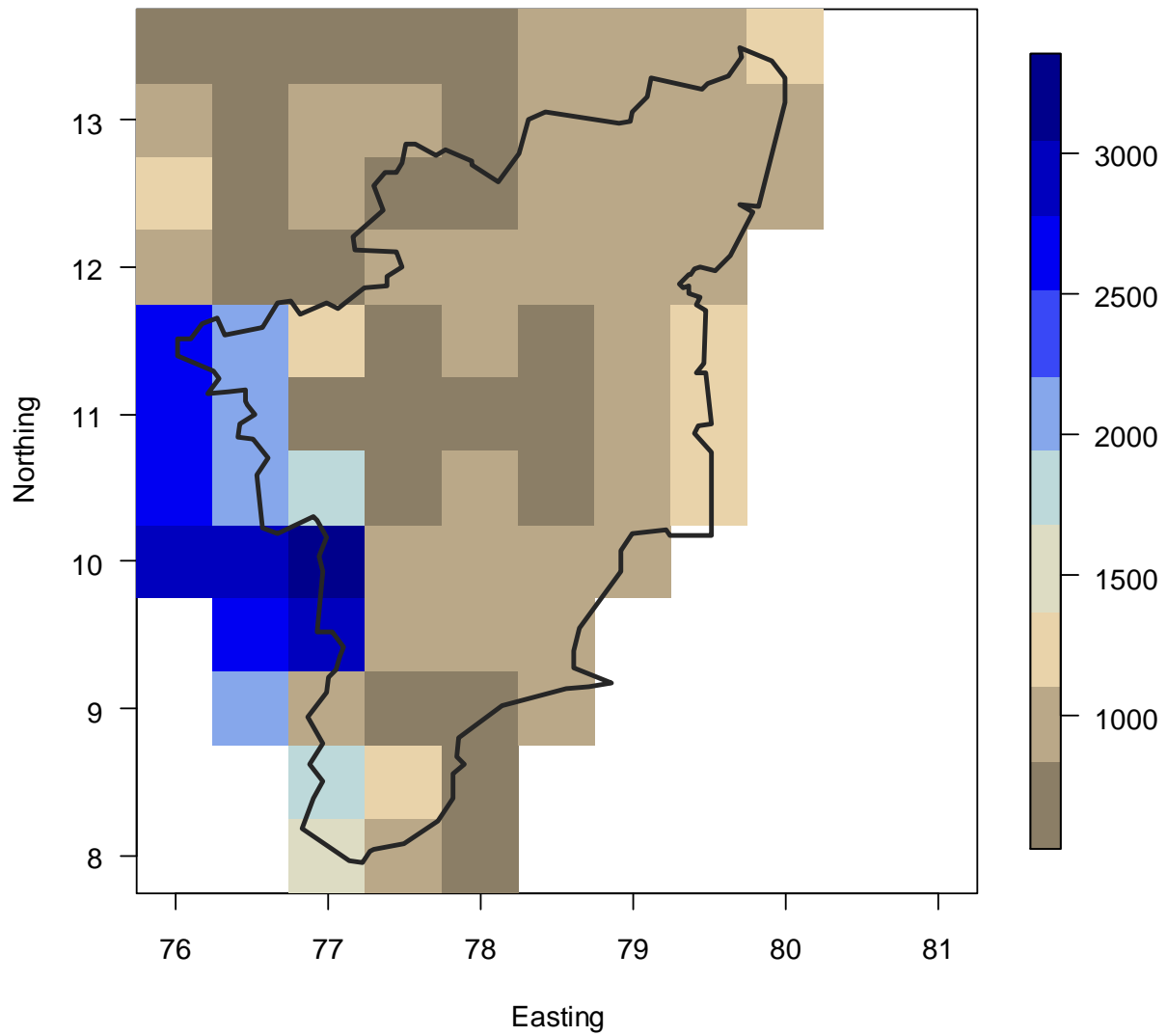


*Figure4.1: 24-Years Mean Annual Rainfall Variation in Tamil Nadu - Entire state*

**24 year Mean Annual Rainfall Variations in South India,  
1982 - 2005 (mm per year)**

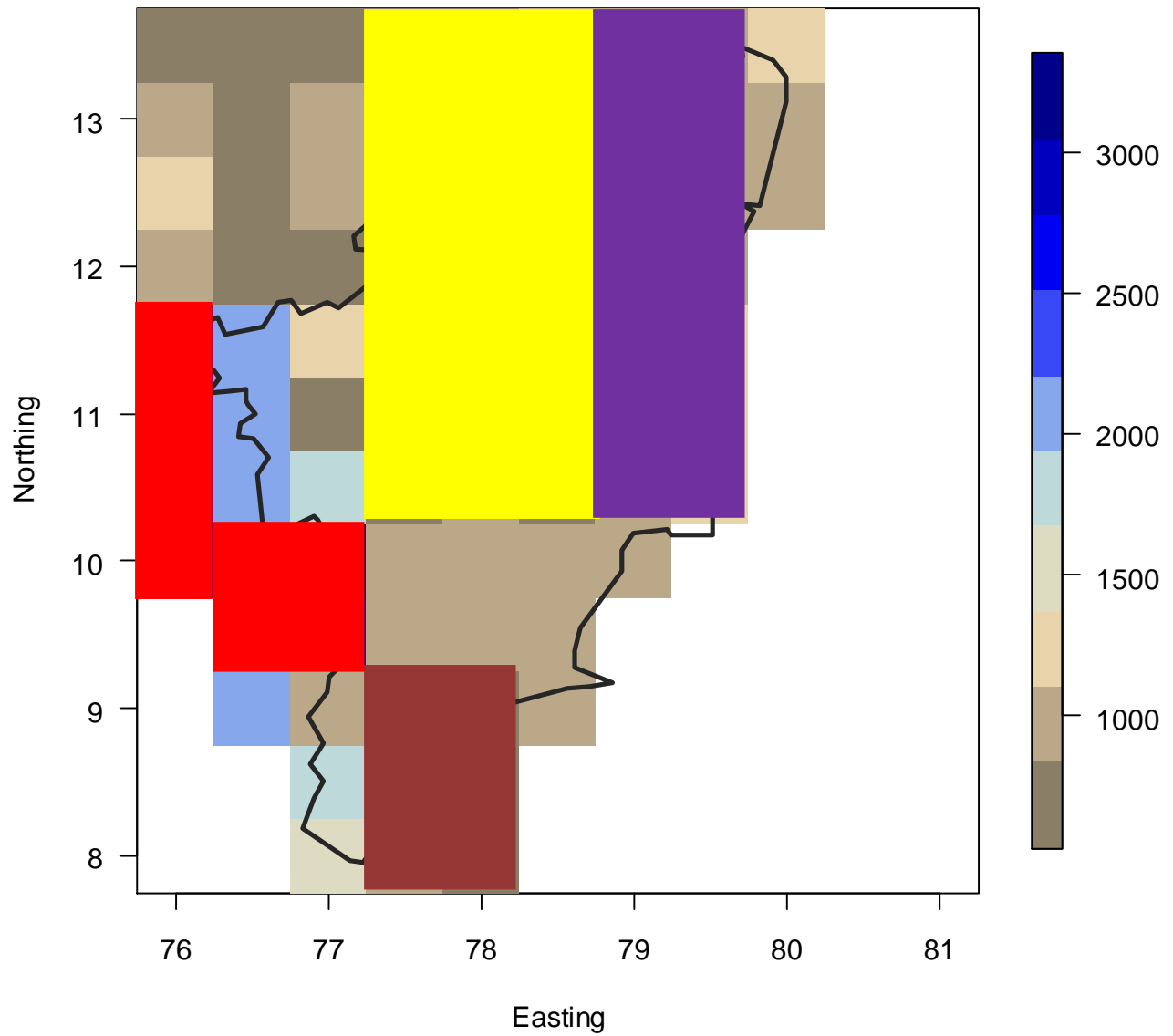


*Figure4.2: 24-Years Mean Annual Rainfall Variation in Tamil Nadu - Domains highlighted*

Table 4.2. Rainfall variation of the four domains in Tamil Nadu based on 24-year mean rainfall

Domain	24-year Mean Rainfall (mm/year)	Latitude (degree N)	Longitude (degree E)
Yellow	>500 & <1000	10.5 – 13.0	77.5 – 78.5
Brown	>700 & <910	8.0 – 9.0	77.5 – 78.0
Purple	>800 & <1210	10.5 – 13	79.0 – 79.5
Red	>2500	10.0 – 11.5; 9.5 – 10.0	76.0; 76.5 – 77.0

These domains were tested for statistically significant differences in their means using one-way repeated measures ANOVA at 95% confidence level. The mean differences were not significant among Yellow, Purple and Brown domains, as illustrated in Table 4.3. This is well depicted by the box plot showing rainfall variations in these four domains. As it can be seen, the median rainfall value does not vary much for the ‘purple’, ‘yellow’, ‘brown’ domains, which led to the merging of these domains based on significant mean differences.

Table 4.3 Pair wise comparisons of Rainfall Variations across all domains in Tamil Nadu

Tukey's Honestly-Significant-Difference Test					
Domains	Domains	Difference	p-Value	95% Confidence Interval	
				Lower	Upper
<b>Purple</b>	Yellow	17.010	0.548	-15.996	50.016
<b>Purple</b>	Brown	15.566	0.619	-17.440	48.572
<b>Purple</b>	Red	-152.104	0.000	-185.109	-119.098
<b>Yellow</b>	Brown	-1.444	0.999	-34.449	31.562
<b>Yellow</b>	Red	-169.113	0.000	-202.119	-136.108
<b>Brown</b>	Red	-167.670	0.000	-200.675	-134.664

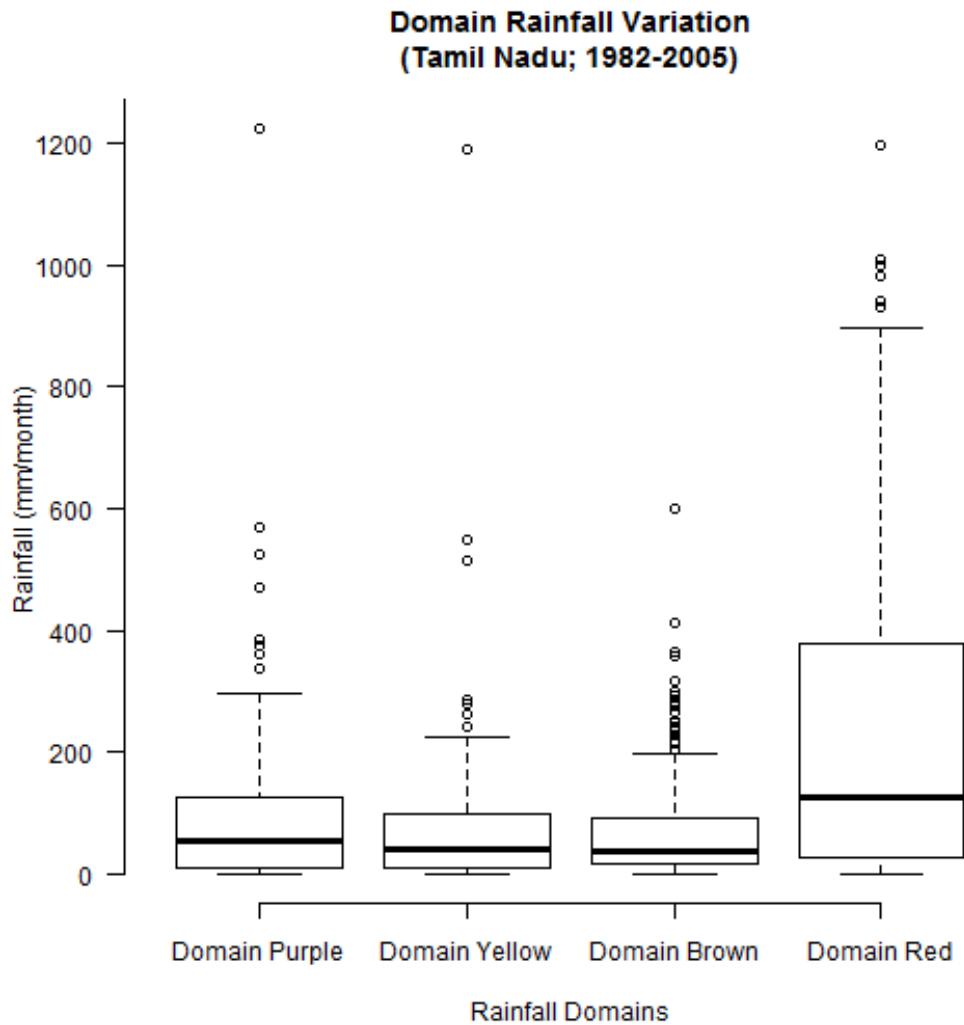


*Figure 4.3: Box plots of Rainfall Variations across all domains in Tamil Nadu*

Thus, two main domains, namely, “TN East” and “TN West” were defined which were also statistically significant at 95% confidence level (Table 4.4) with an F-statistic of  $F(1, 574) = 99.69$  at  $p\text{-value} = 0.000$  obtained from a ‘One-way repeated measures ANOVA’. The Box plots (Figure 4.4) also emphasize their rainfall value differences. In this way, I have identified areas that are statistically coherent.

Table 4.4 Pair wise comparisons of Rainfall Variations across the final domains in Tamil Nadu

Tukey's Honestly-Significant-Difference Test					
Domains	Domains	Difference	p-Value	95% Confidence Interval	
				Lower	Upper
TN East	TN West	-162.309	0.000	-194.171	-130.448

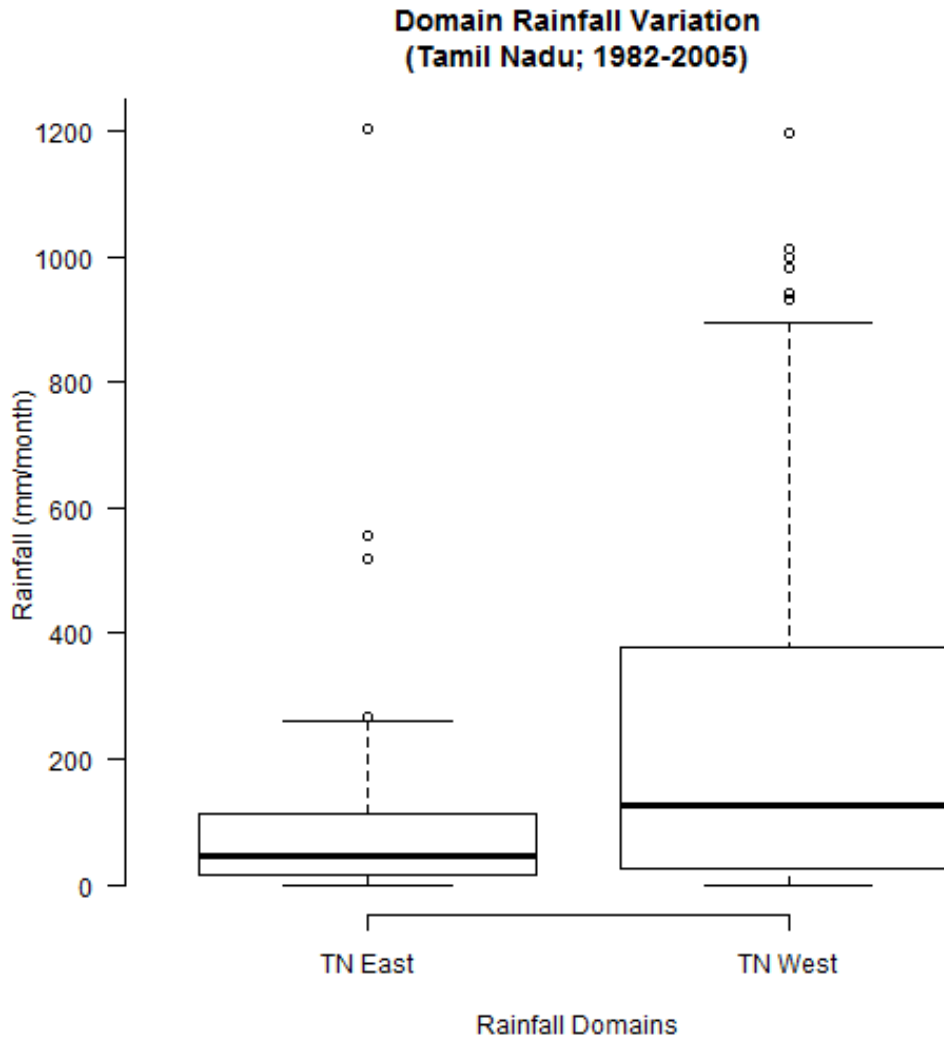


Figure 4.4: Box plots of Rainfall Variations across the final domains in Tamil Nadu

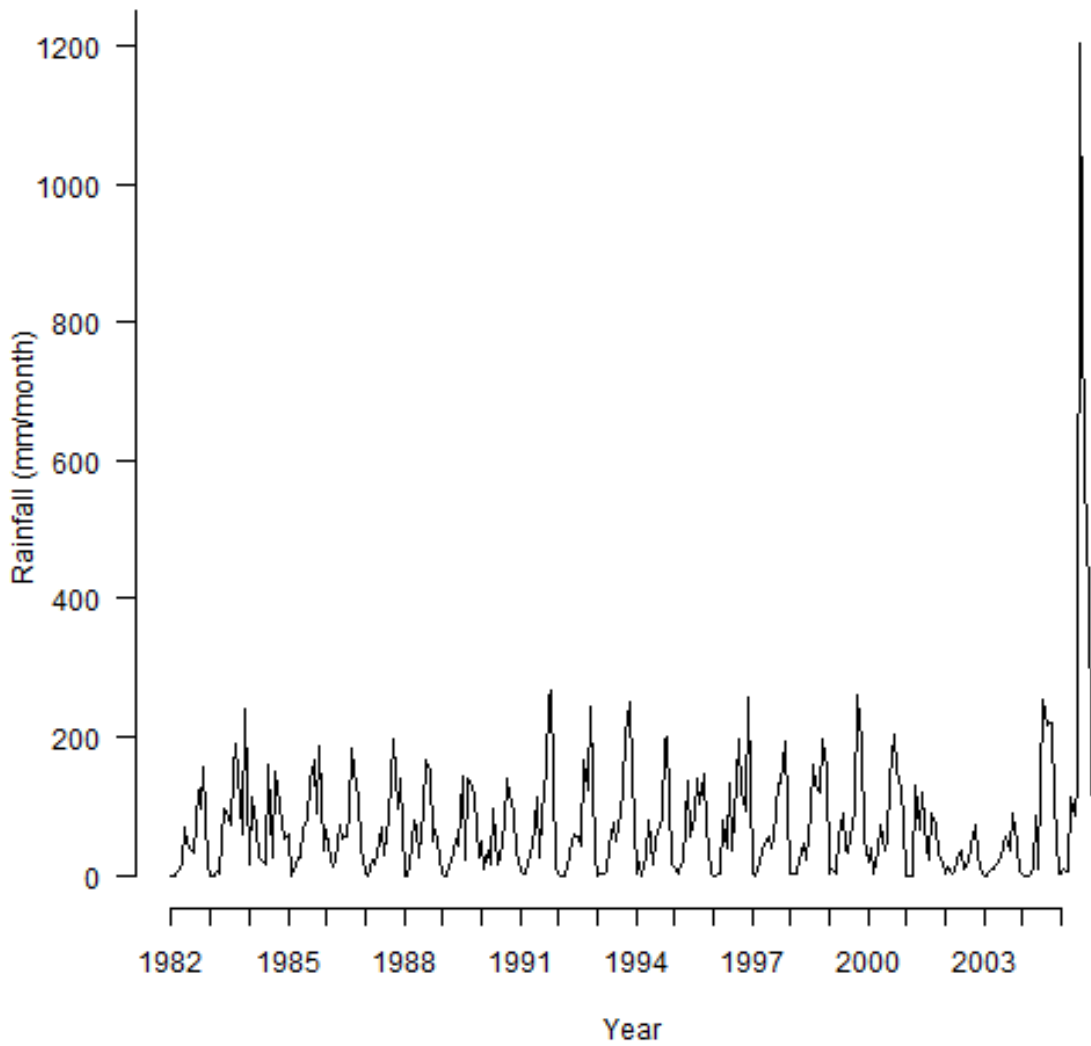
## **4.2 Time Series Analysis & Analysis of Variance**

The monthly values obtained for each phenomenon over the 24 year period, 1982 – 2005, were analyzed using time series plots. These plots in combination with the regional precipitation box plots help describe the patterns of each phenomenon over the study period. These are needed to identify and account for the periodic phenomena that may affect the anomalous rainfall event in 2004.

### **4.2.1 Rainfall Pattern**

From the time series plot of monthly rainfall variations in TN East domain (Figure 4.5), a seasonal rainfall cycle is evident which repeats itself every year and in some cases repeats with less intensity. Except for 2005, this seasonal cycle has been mostly similar through TN East domain. Whereas, TN West's time series plot is quite moderate throughout the 24 year study period without much deviations from the mean. These seasonal variations almost inhibit further analysis of these plots and the monthly variations in these domains are hidden in these time series plots which compelled for their rigorous analysis via box plots.

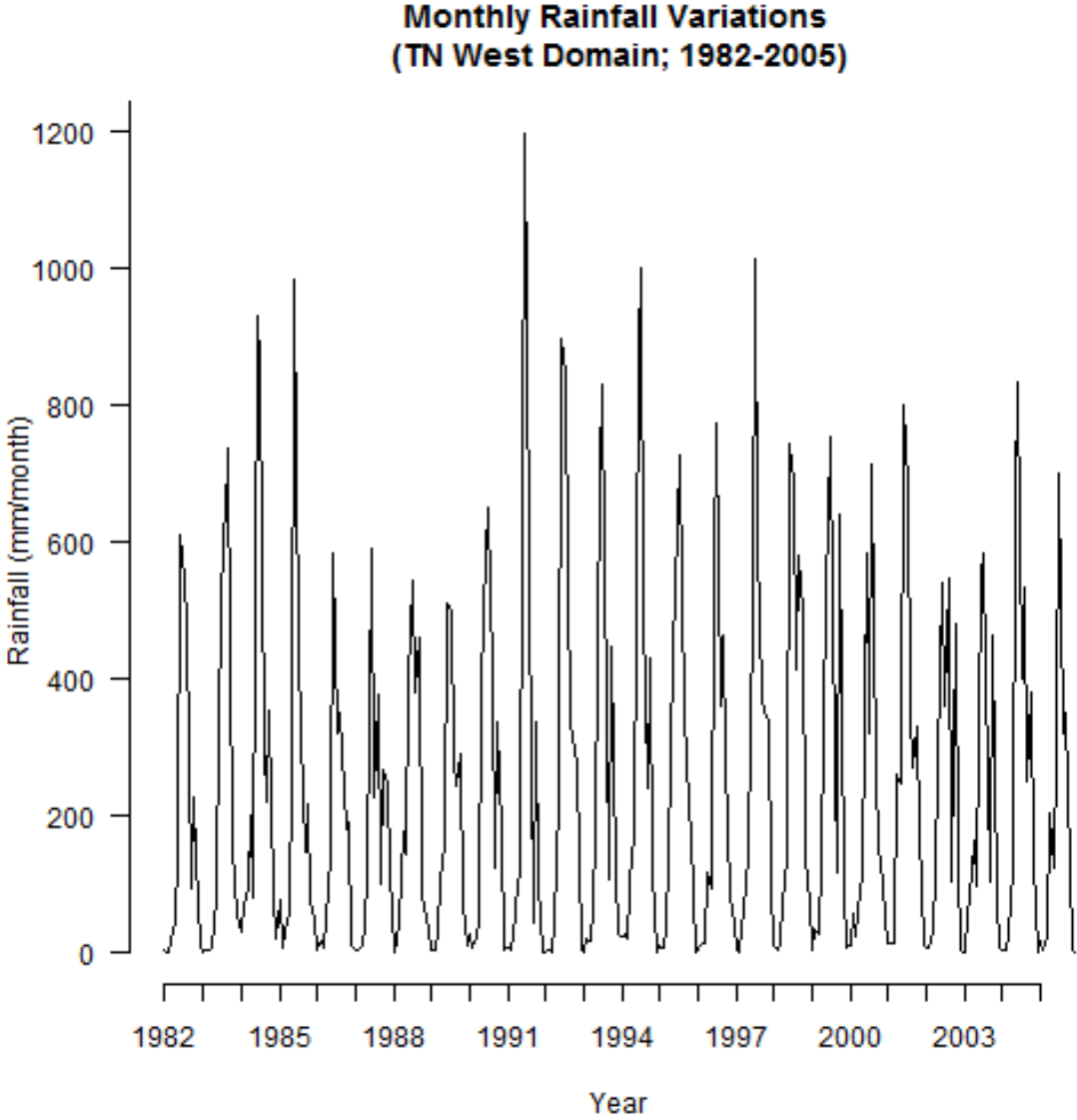
**Monthly Rainfall Variations  
(TN East Domain; 1982-2005)**



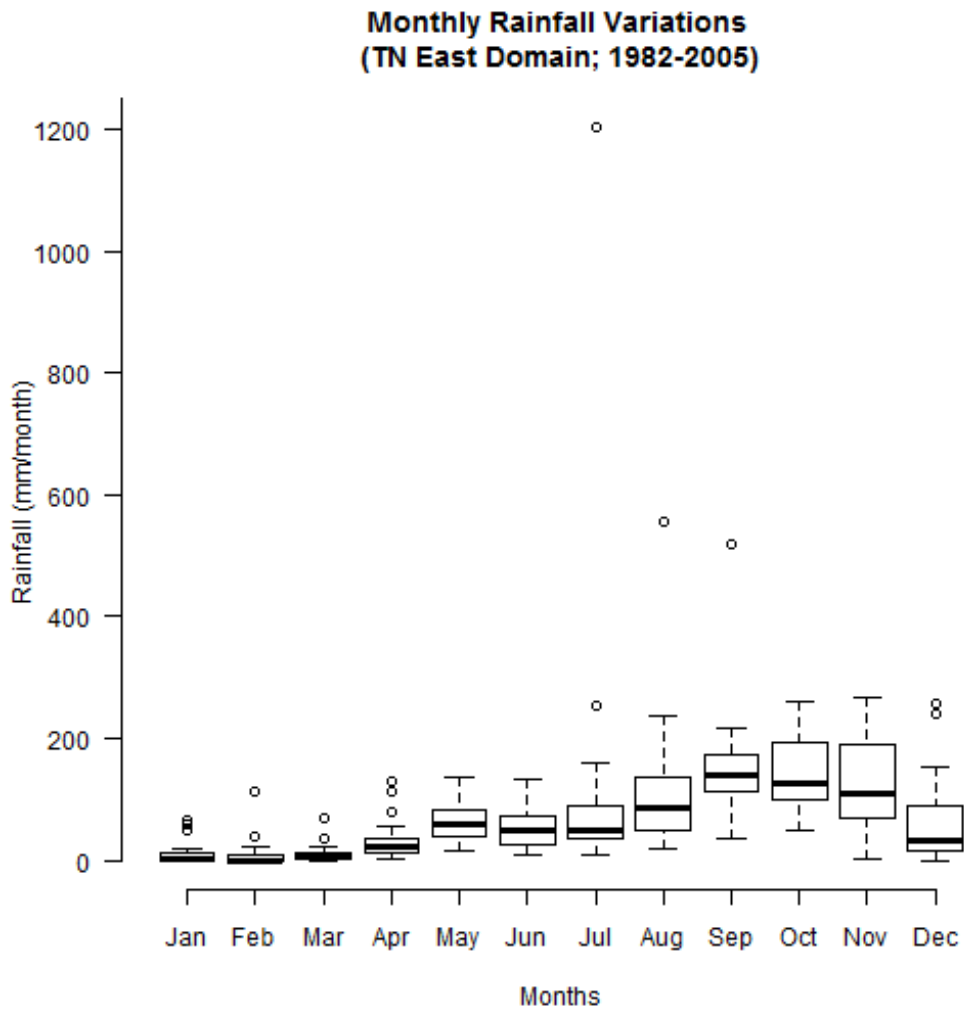
(a)

*Figure 4.5: Time Series plots of Monthly Rainfall Variations for the period 1982 – 2005 (a) TN East Domain (b) TN West Domain*

Figure 4.5(cont'd) Time Series plots of Monthly Rainfall Variations for the period 1982 – 2005  
(a) TN East Domain (b) TN West Domain



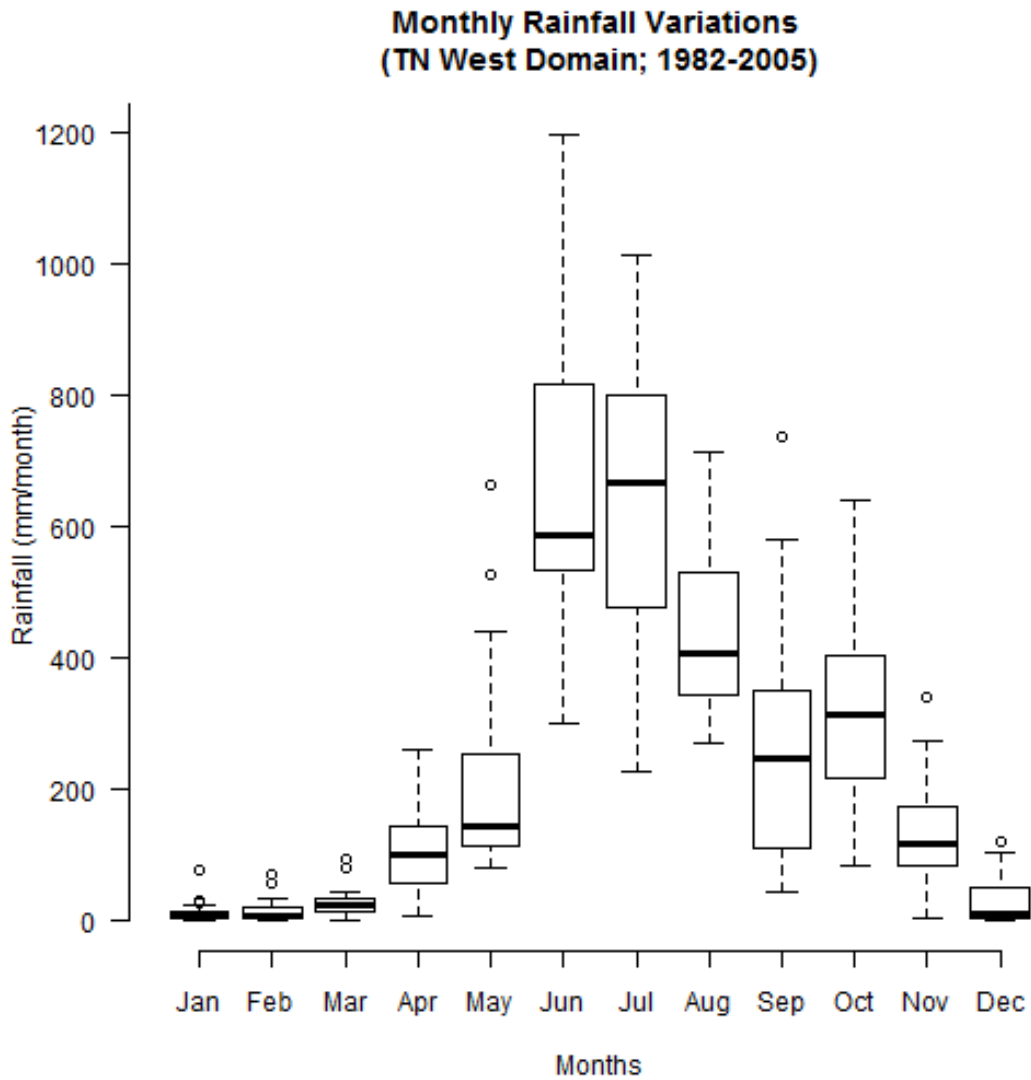
(b)



(a)

Figure 4.6: Box plots of Monthly Rainfall Variations for the period 1982 – 2005 (a) TN East Domain (b) TN West Domain

Figure 4.6 (cont'd) Box plots of Monthly Rainfall Variations for the period 1982 – 2005 (a) TN East Domain (b) TN West Domain



(b)

Box plot of the TN East domain (Figure 4.6 (a)) demonstrates a bimodal (two peaks) rainfall variation present in this domain. Although, the first peak is not very clear in the plot, the Inter quartile range (IQR, 50% of rainfall in a month) for this domain (Table 4.5) clearly reveals the

monthly rainfall peaks obtained once in summer (June or July) and another in winter (October or November).

*Table 4.5 Inter Quartile Range (IQR) values for rainfall domains in Tamil Nadu*

<b>Month</b>	<b>IQR - TN East (mm per month)</b>	<b>IQR - TN West (mm per month)</b>
January	10.82	9.79
February	9.27	15.96
March	12.54	17.62
April	21.86	89.67
May	44.38	140.48
June	48.10	281.77
July	52.96	325.77
August	89.80	188.76
September	62.67	239.14
October	94.85	188.83
November	121.99	91.09
December	72.32	45.08

In contrast, TN West domain depicts a clear unimodal (single peak) rainfall variation through the box plot of monthly rainfall variations (Figure 4.6 (b)). This is further supported by the IQR values obtained for TN West (Table 4.5). This can be explained by the proximity of Western domain to the Western Ghats of South India which help bring SWMR in the months of June – September for most parts of the country (Revadekar and Kulkarni, 2008).

### 4.2.2 SST Pattern

One way repeated measures ANOVA resulted in significant differences among the SST regions used in this research study. These regions were statistically significant with an F-statistic,  $F(4, 1435) = 677.462$  at  $p\text{-value} = 0.000$ . This is illustrated by the box plot (Figure 4.7) showing differences in SST values among these regions and the pair-wise comparisons results obtained from Tukey's Honestly-Significant-Difference test (Table 4.6)

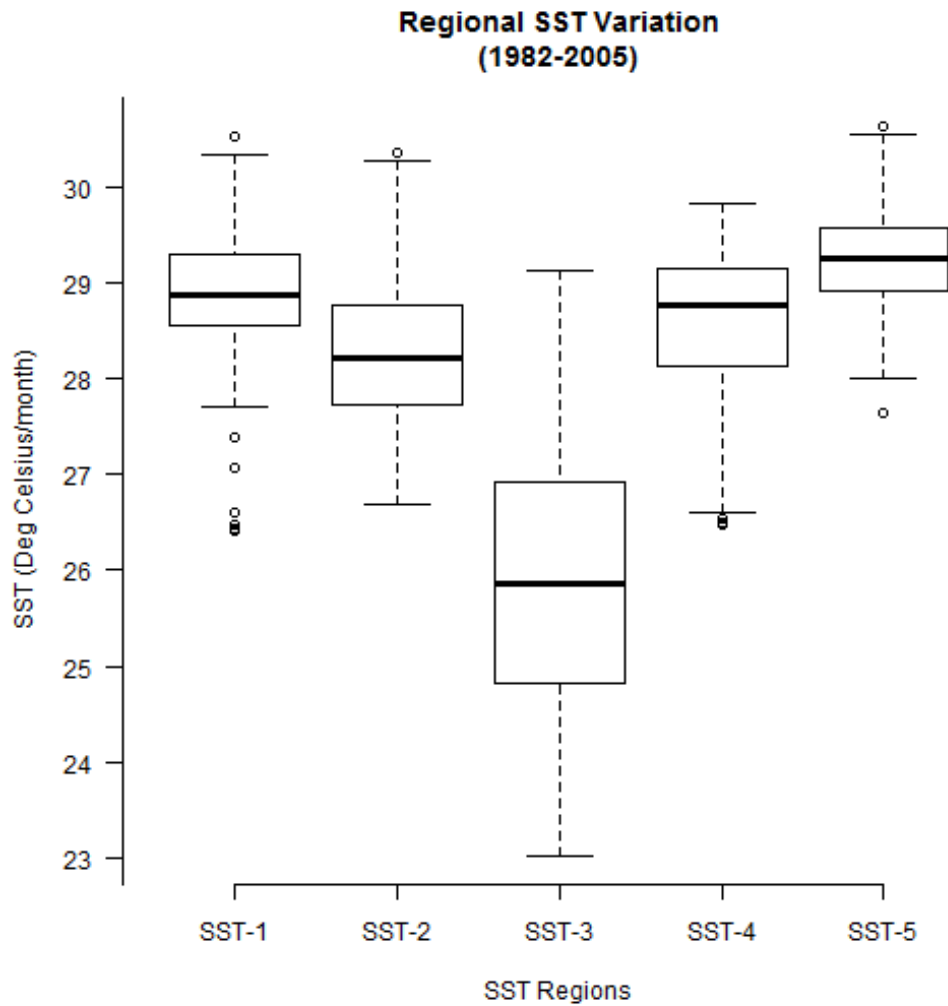
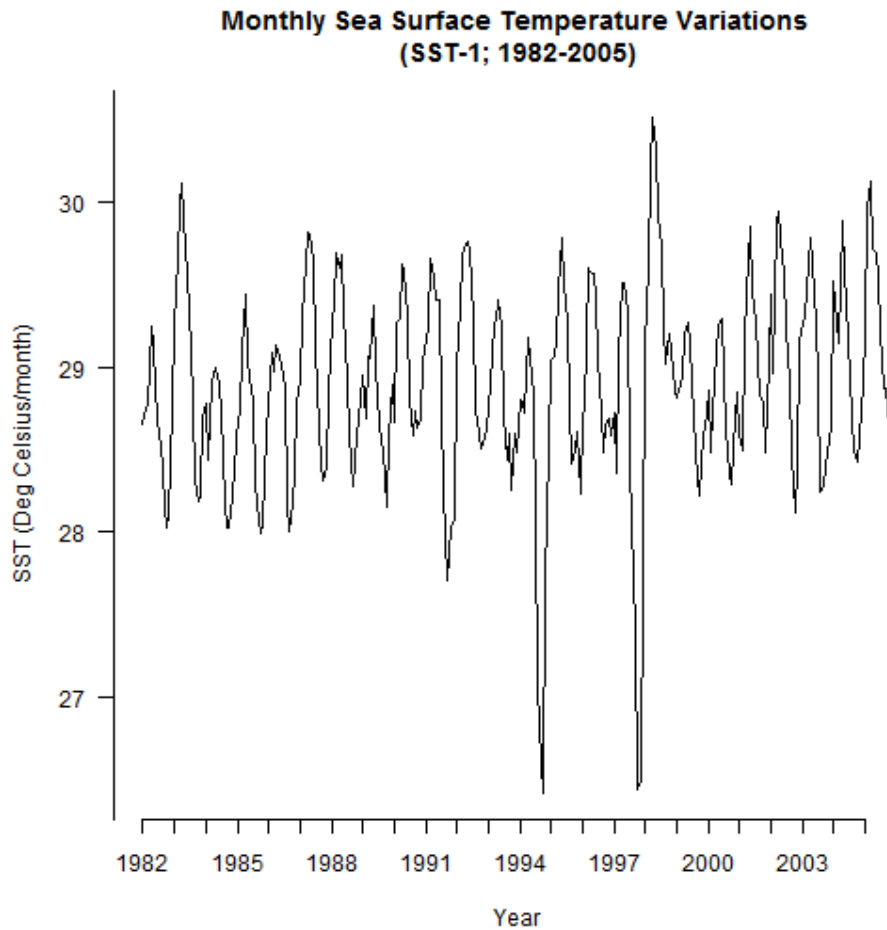


Figure 4.7: Box plot of SST Variations across all regions for the period 1982 – 2005

Table 4.6 Pair wise comparisons of SST Variations across all regions (1982 – 2005)

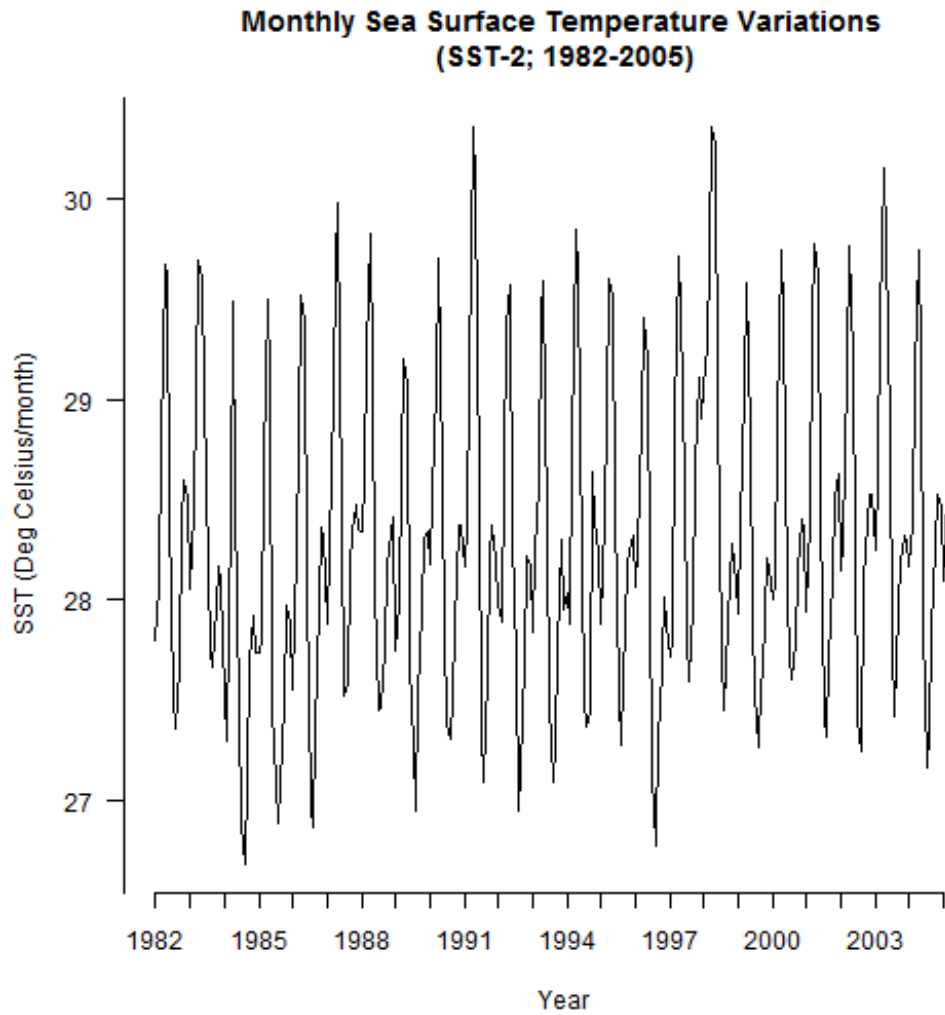
Tukey multiple comparisons of means						
Region\$(i)\$	Region\$(j)\$	Difference	95% Confidence Interval		p-Value	
			Lower	Upper		
SST 1	SST 2	-0.577	-0.772	-0.382	0.000	
SST 1	SST 3	-2.943	-3.138	-2.748	0.000	
SST 1	SST 4	-0.291	-0.487	-0.096	0.000	
SST 1	SST 5	0.367	0.172	0.562	0.000	
SST 2	SST 3	-2.366	-2.561	-2.171	0.000	
SST 2	SST 4	0.286	0.090	0.481	0.001	
SST 2	SST 5	0.944	0.749	1.139	0.000	
SST 3	SST 4	2.651	2.456	2.847	0.000	
SST 3	SST 5	3.310	3.115	3.505	0.000	
SST 4	SST 5	0.659	0.463	0.854	0.000	



(a)

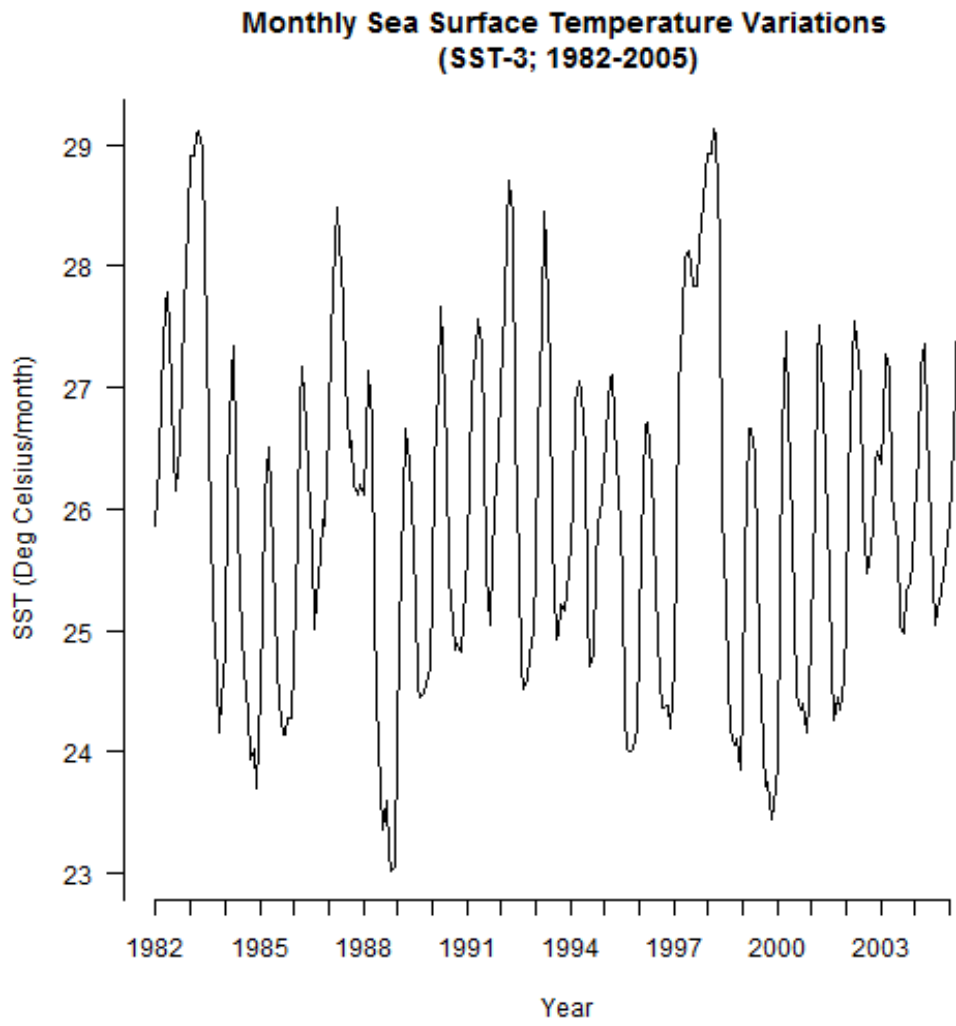
Figure 4.8: Time Series plots of SST Variations for each region (1982 – 2005); (a) SST-1 region; (b) SST-2 region; (c) SST-3 region; (d) SST-4 region; (e) SST-5 region

Figure 4.8 (cont'd) Time Series plots of SST Variations for each region (1982 – 2005); (a) SST-1 region; (b) SST-2 region; (c) SST-3 region; (d) SST-4 region; (e) SST-5 region



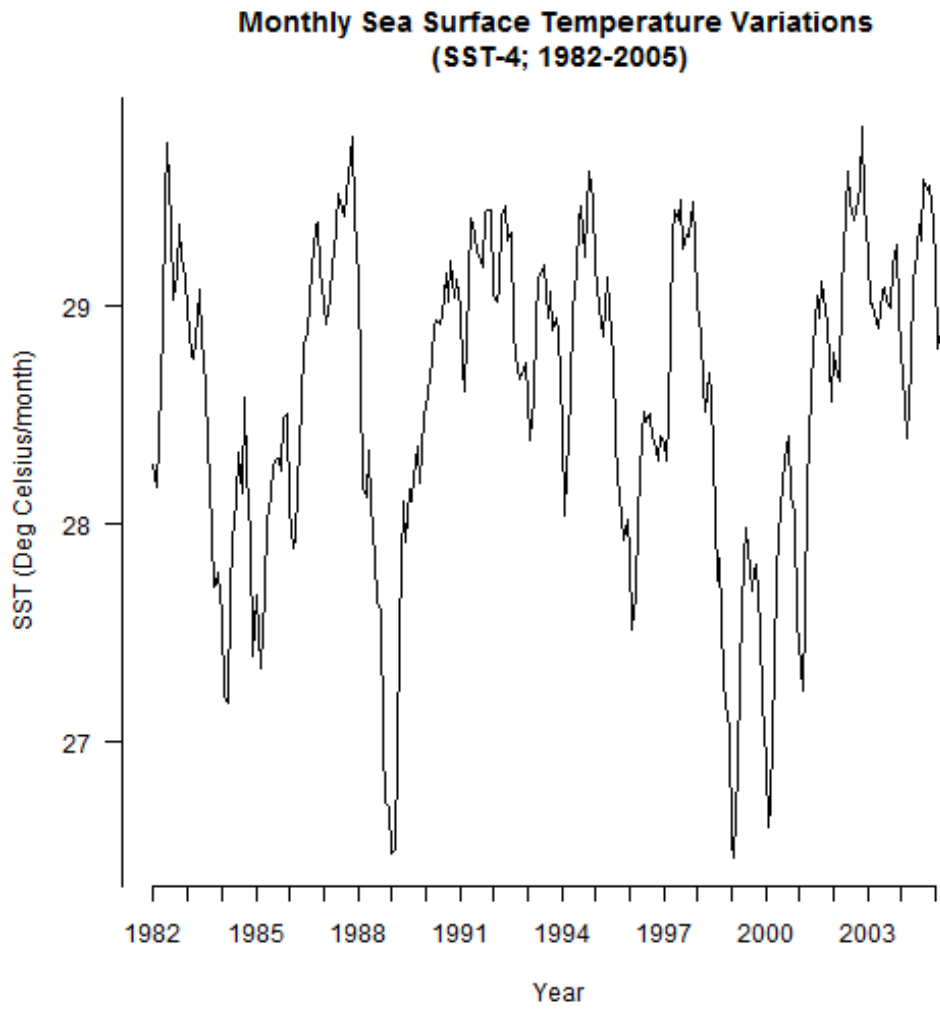
(b)

Figure 4.8 (cont'd) Time Series plots of SST Variations for each region (1982 – 2005); (a) SST-1 region; (b) SST-2 region; (c) SST-3 region; (d) SST-4 region; (e) SST-5 region



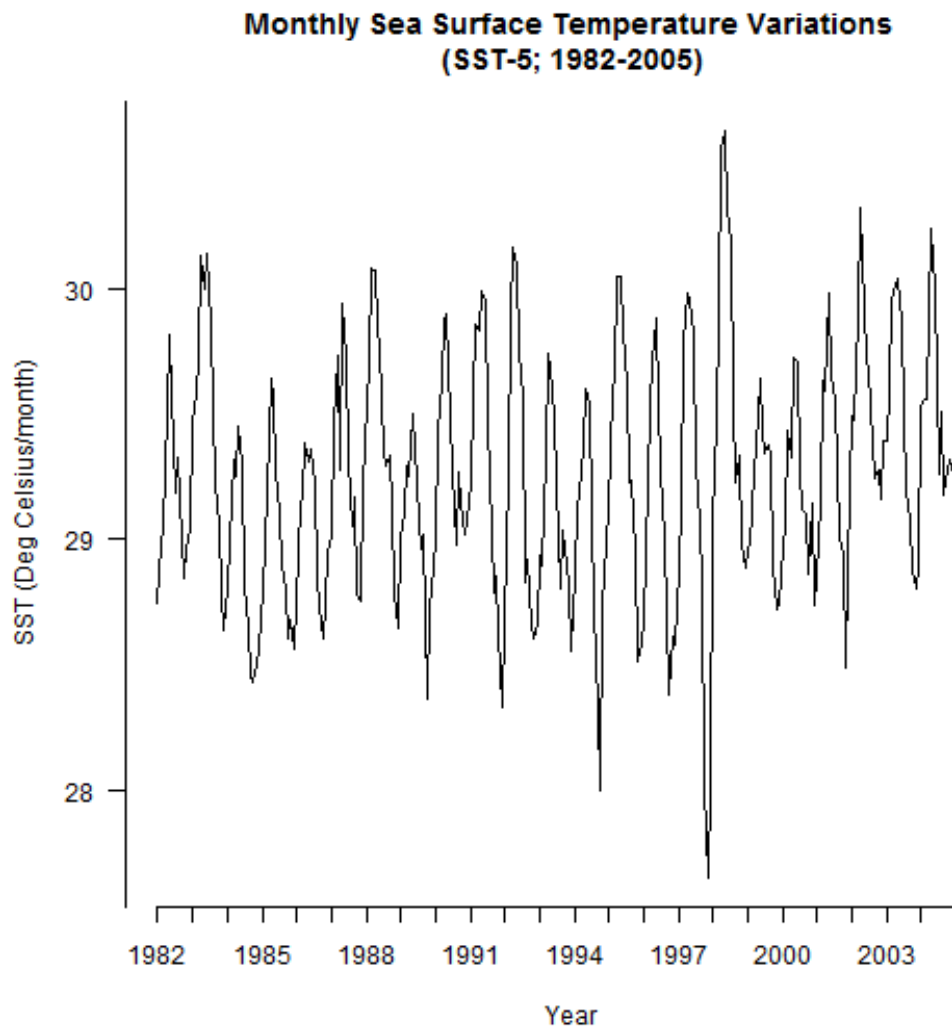
(c)

Figure 4.8 (cont'd) Time Series plots of SST Variations for each region (1982 – 2005); (a) SST-1 region; (b) SST-2 region; (c) SST-3 region; (d) SST-4 region; (e) SST-5 region



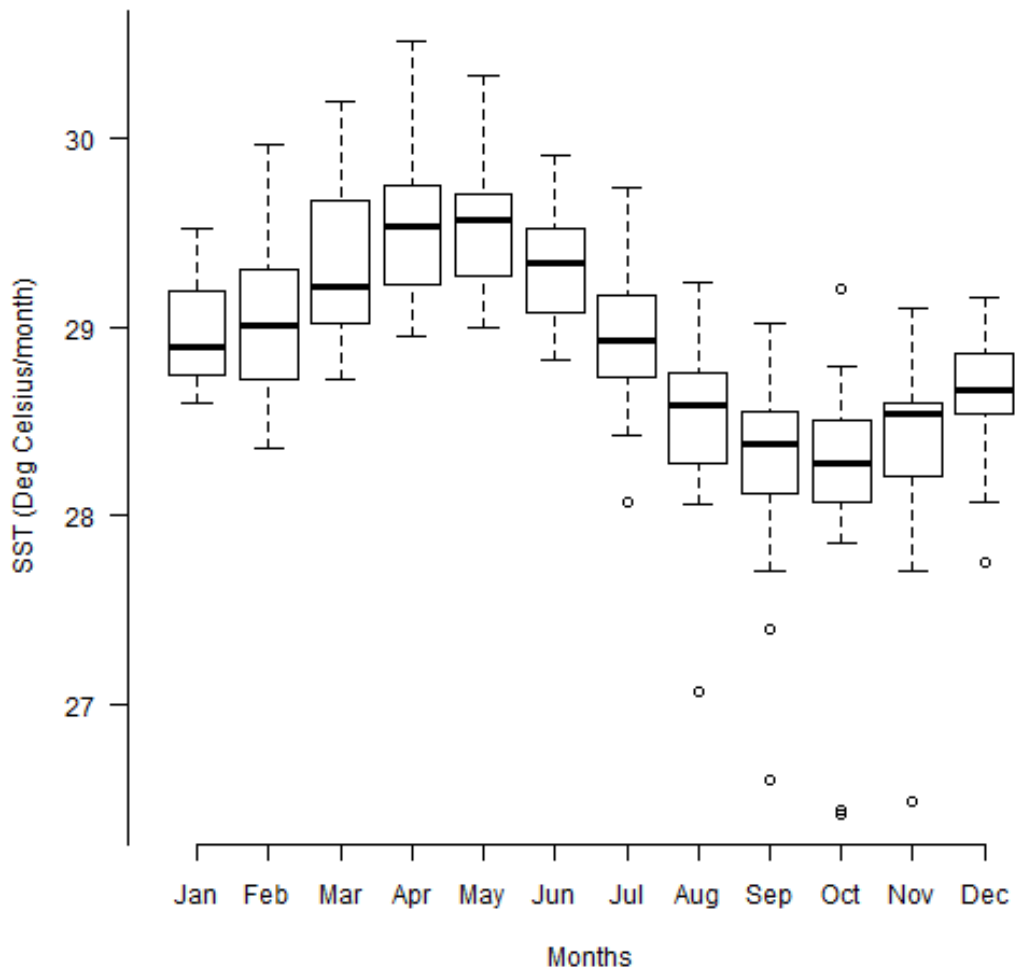
(d)

Figure 4.8 (cont'd) Time Series plots of SST Variations for each region (1982 – 2005); (a) SST-1 region; (b) SST-2 region; (c) SST-3 region; (d) SST-4 region; (e) SST-5 region



(e)

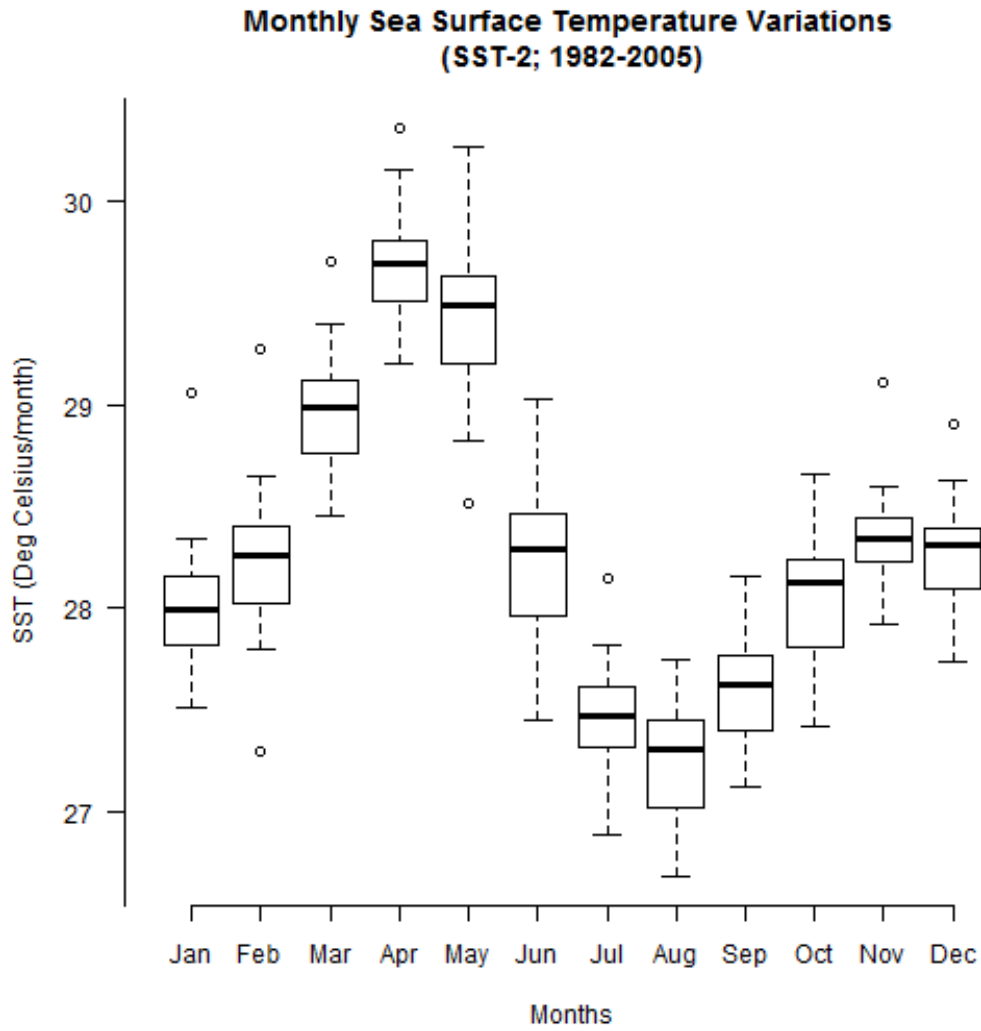
**Monthly Sea Surface Temperature Variations  
(SST-1; 1982-2005)**



(a)

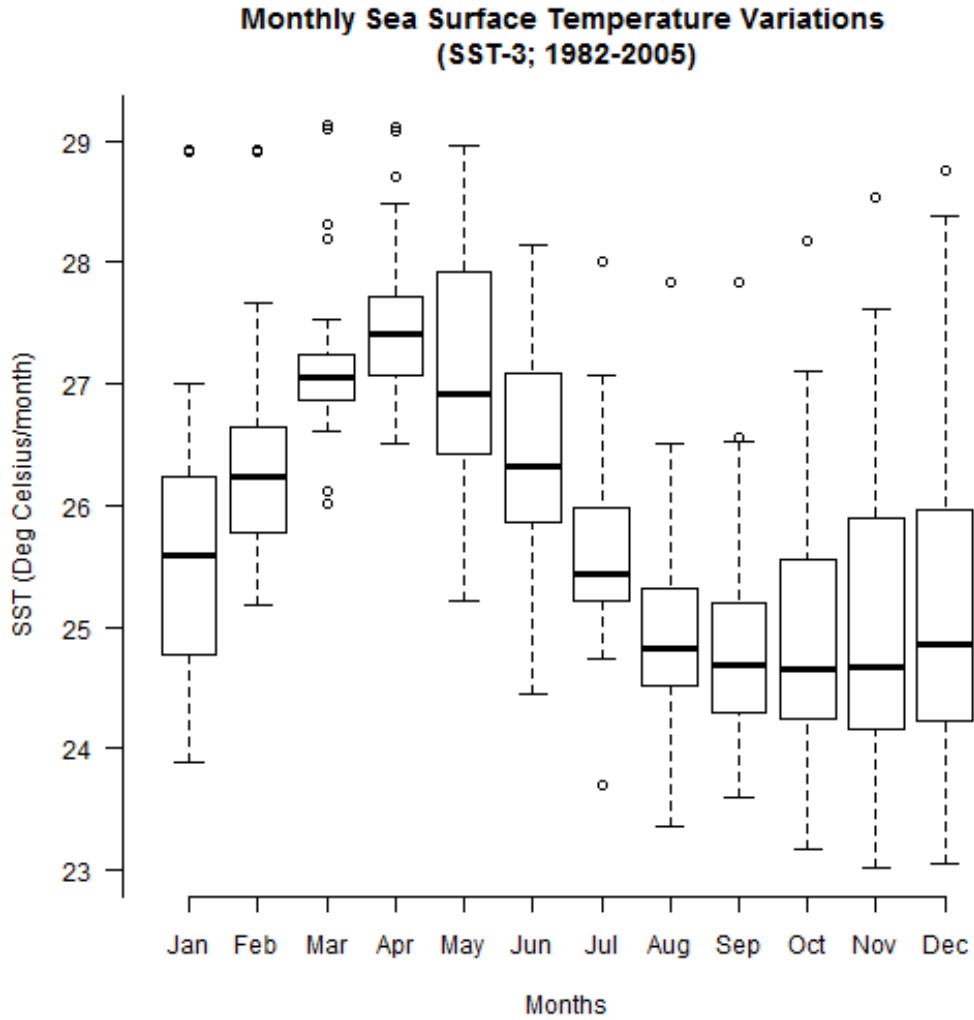
*Figure 4.9: Box plots of SST Variations for each region (1982 – 2005); (a) SST-1 region; (b) SST-2 region; (c) SST-3 region; (d) SST-4 region; (e) SST-5 region*

Figure 4.9 (cont'd) Box plots of SST Variations for each region (1982 – 2005); (a) SST-1 region; (b) SST-2 region; (c) SST-3 region; (d) SST-4 region; (e) SST-5 region



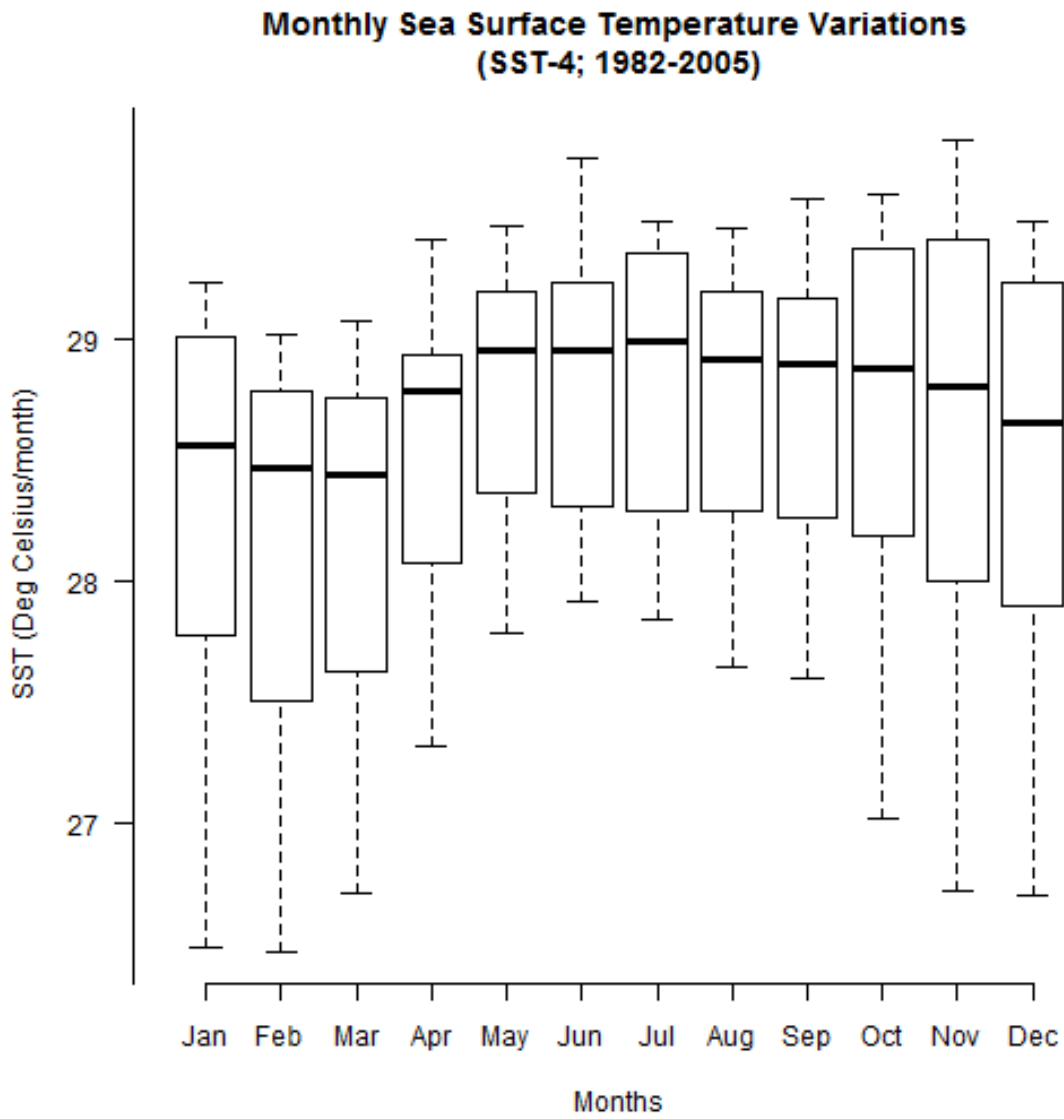
(b)

Figure 4.9 (cont'd) Box plots of SST Variations for each region (1982 – 2005); (a) SST-1 region; (b) SST-2 region; (c) SST-3 region; (d) SST-4 region; (e) SST-5 region



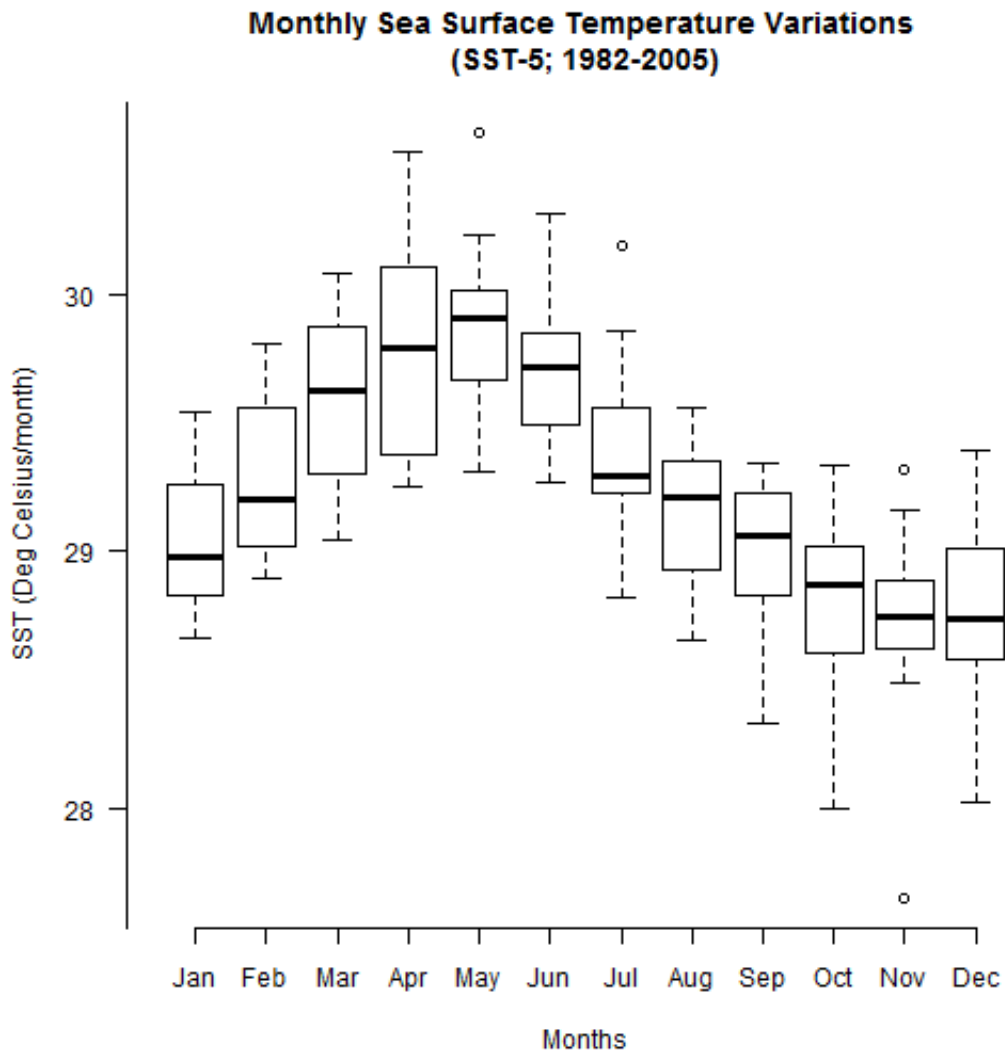
(c)

Figure 4.9 (cont'd) Box plots of SST Variations for each region (1982 – 2005); (a) SST-1 region; (b) SST-2 region; (c) SST-3 region; (d) SST-4 region; (e) SST-5 region



(d)

Figure 4.9 (cont'd) Box plots of SST Variations for each region (1982 – 2005); (a) SST-1 region; (b) SST-2 region; (c) SST-3 region; (d) SST-4 region; (e) SST-5 region



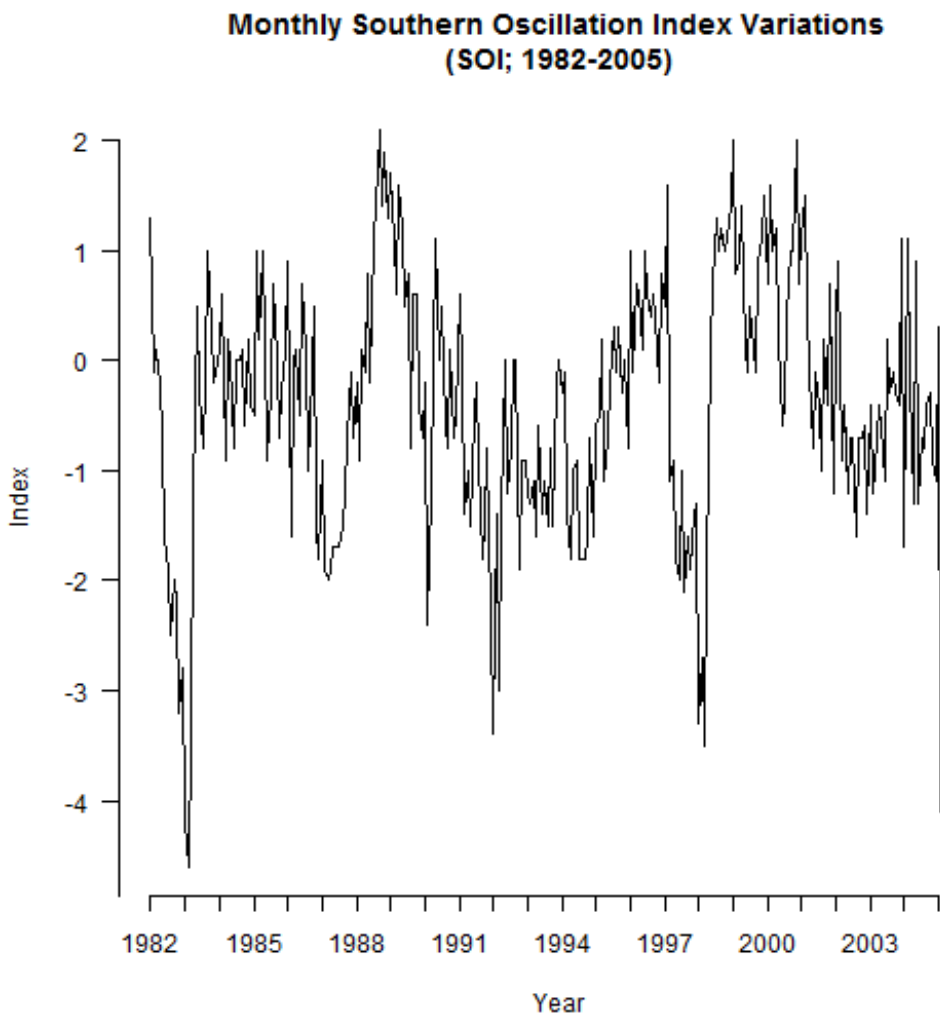
(e)

This was followed by further time-series (Figure 4.8) and box plot analyses (Figure 4.9) for these regions. These plots were compared to those of SOI and DMI to understand the general behavior of these phenomena in comparison with one another.

These plots illustrate that eastern and western parts of the Indian Ocean have a minimum of 27.9, 26.7 and a maximum of 30.5, 30.2 degree Celsius per month respectively. While the eastern and

western parts of the Pacific Ocean have a minimum of 23.0, 26.5 and a maximum of 29.0, 29.8 degree Celsius per month respectively. Although the maximum temperatures were quite similar for these regions, there is at least a one to three degree Celsius temperature difference per month implying different temperature changes in these regions might have different effect over the global monsoon pattern.

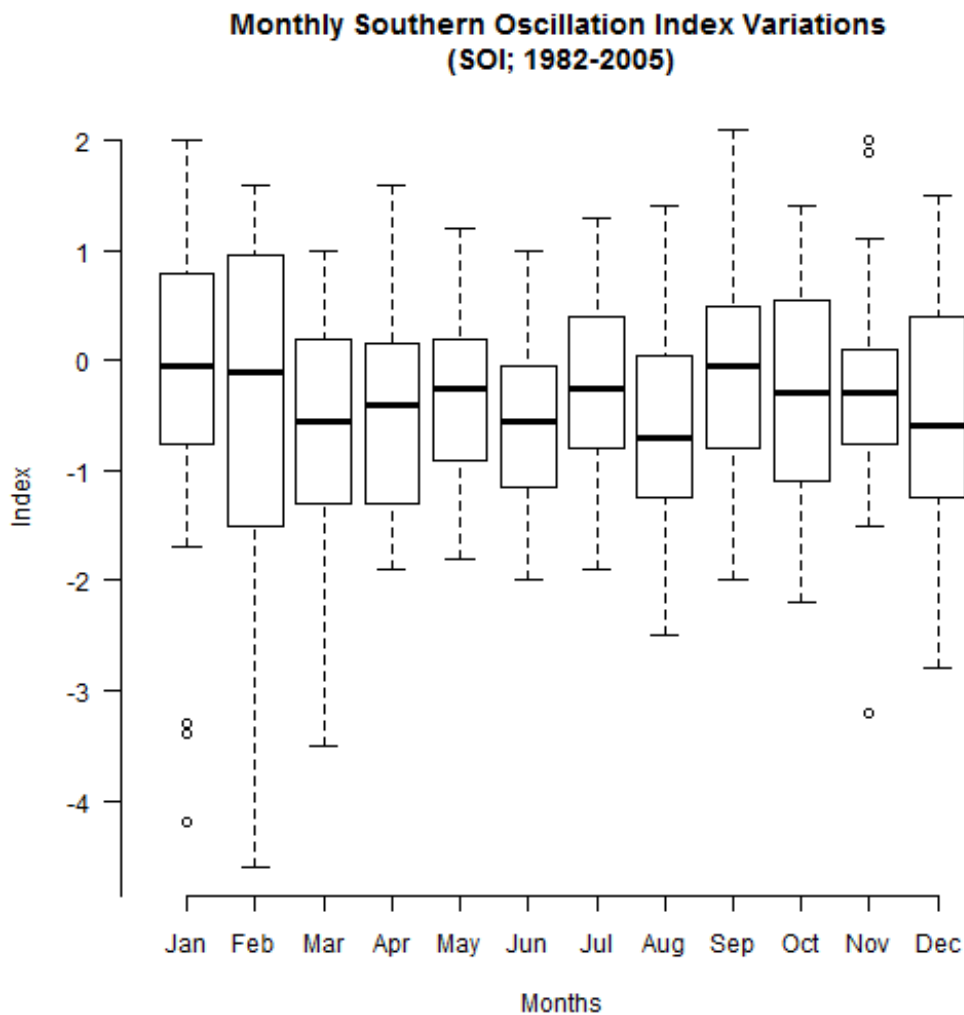
### 4.2.3 SOI Pattern



(a)

*Figure 4.10: Southern Oscillation Index Variation (1982 – 2005) (a) Time Series plot (b) Box plot*

Figure 4.10 (cont'd) Southern Oscillation Index Variation (1982 – 2005) (a) Time Series plot (b) Box plot



(b)

The time series plot (Figure 4.10 (a)) of SOI index clearly depicts the highs and lows of ENSO phenomenon observed during the study period. As can be evidently seen, SOI has a minimum of -4.6, while a maximum of 2.1 meaning a strong El-Nino event occurred in the years 1982-83, and a La-Nina event in the year 1988 (Meyers G. et. al., 2006).

#### 4.2.4 DMI Pattern

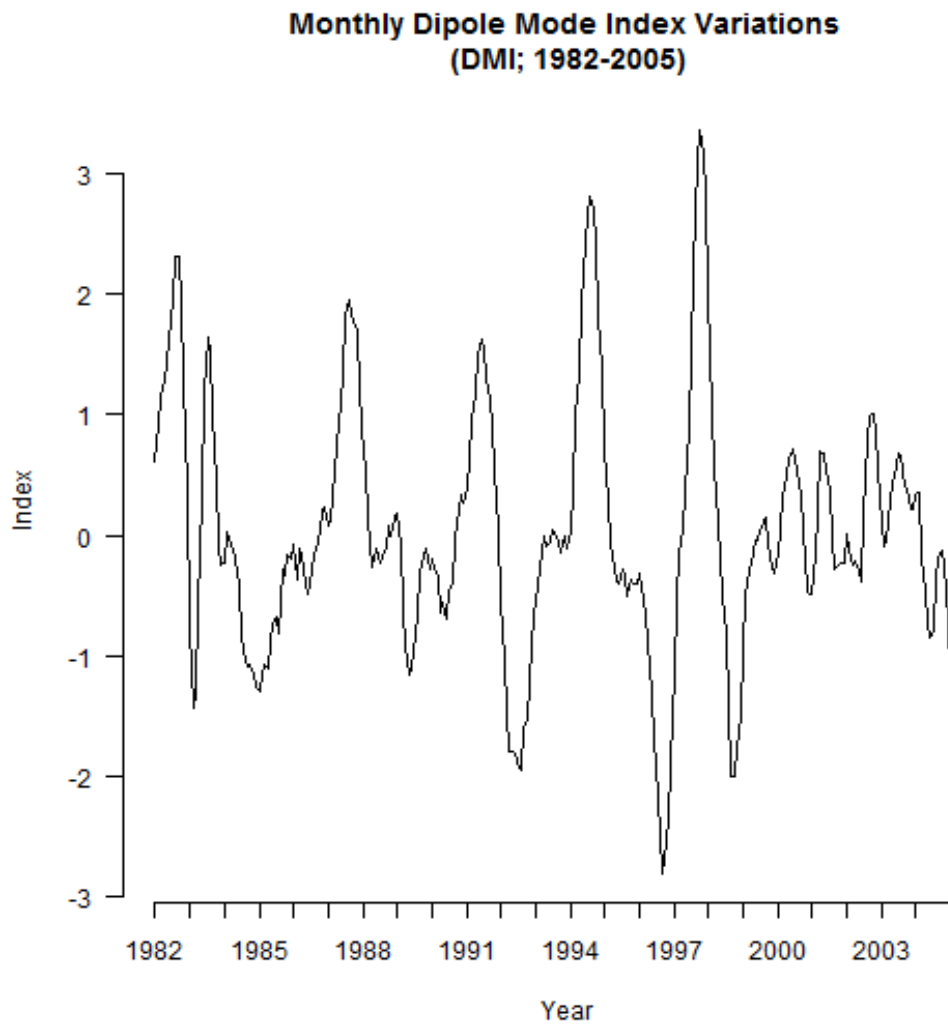
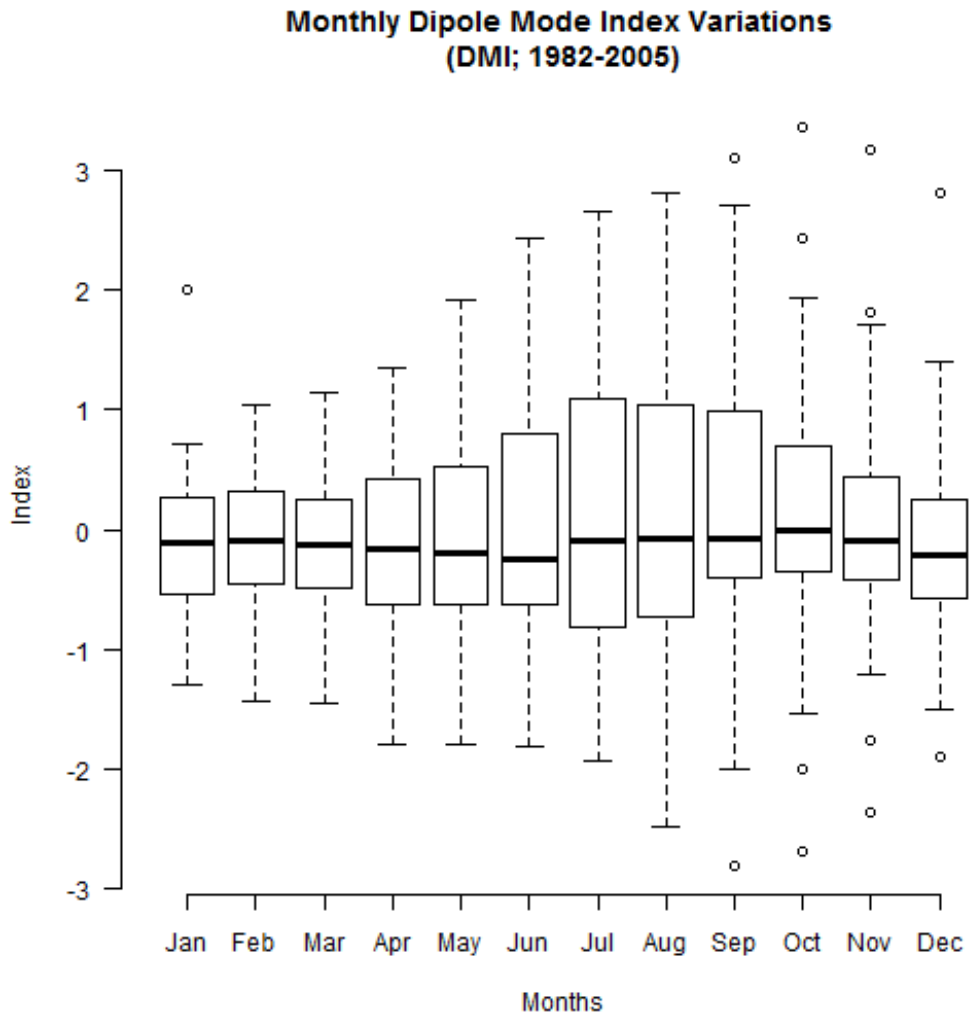


*Figure 4.11: Dipole Mode Index Variations (1982 – 2005) (a) Time Series plot (b) Box plot*

Figure 4.11(cont'd) Dipole Mode Index Variations (1982 – 2005) (a) Time Series plot (b) Box plot



(b)

The DMI time series plot (Figure 4.11 (a)) illustrates a minimum of -2.5 and a maximum of 2.8 observed during a negative event in 1996 and a positive event in 1994 respectively (Meyers G., et. al., 2006). Further, these plots emphasize the irregular nature of IOD event' presence in Indian Ocean, thereby implying the complex nature of this ocean-atmosphere coupling phenomenon.

### 4.3 Time-lag Correlation

This analysis helps understand the lag correlation that exists between different phenomena considered in this research. It resulted in a big matrix (12x7) of correlation values between each factor considered and rainfall in a particular domain in the study area. The correlation value cells are marked in light gray (with *italic* font) and dark gray (with **bold** font) colors as per their 90% and 95% confidence levels respectively. Thus, for a single rainfall domain, three such matrices were obtained, one for each month in NEMR period. In total, six such matrices were obtained for both the domains. The main point to be noted in these correlation matrices is the lag between the significant correlations and the NEMR period which will be focused chiefly in the following analyses sections.

#### 4.3.1 Rainfall Domain – TN East

For TN East domain, October correlation matrix (Table 4.7 (a)) did not have any significant correlation values except September' SOI values, while November had significant correlations (at 90% and 95% confidence value) for SOI, SST-1 SST-2, SST-5, and December had significant correlations for SOI and SST-3. Thus, November rainfall (Table 4.7 (b)) in TN East domain is mostly correlated with short lags of SOI, SST-1, SST-2 (i.e. for SOI and SST values in August, September and October) and long lags of SST-5 values. Whereas, December rainfall (Table 4.7 (c)) in TN East domain is mostly correlated with long lags of SOI and SST-3 values (i.e. for the months of January, February, March...etc).

Table 4.7 Time-lag Correlation matrices for TN East Rainfall Domain (a) October rainfall (b) November rainfall (c) December rainfall

(a)

	Jan	Feb	Mar	Apr	May	June	July	Aug	Sep	Oct	Nov	Dec
DMI	-0.13	0.04	0.17	0.17	0.19	0.18	0.13	0.11	0.09	0.06	0.04	-0.03
SOI	0.10	-0.04	0.03	-0.21	-0.24	-0.10	-0.17	-0.21	-0.36	-0.06	-0.01	-0.08
SST-1	0.11	0.15	-0.10	-0.15	-0.15	-0.05	-0.14	-0.23	-0.18	-0.17	-0.01	-0.28
SST-2	-0.04	-0.05	-0.13	0.15	0.17	-0.04	-0.07	0.04	-0.03	0.05	0.07	-0.22
SST-3	-0.10	-0.12	-0.09	0.01	0.19	0.21	0.19	0.08	0.02	0.09	0.04	0.06
SST-4	-0.04	-0.06	0.01	0.06	0.10	0.12	0.16	0.18	0.19	0.24	0.20	0.17
SST-5	0.02	0.02	-0.11	-0.16	0.03	0.08	-0.13	0.02	-0.03	-0.07	0.04	-0.15

(b)

	Jan	Feb	Mar	Apr	May	June	July	Aug	Sep	Oct	Nov	Dec
DMI	0.03	0.11	0.20	0.15	0.15	0.15	0.14	0.13	0.17	0.15	0.17	0.18
SOI	-0.14	0.17	-0.26	-0.17	-0.11	-0.28	-0.23	-0.10	-0.41	-0.50	-0.18	-0.15
SST-1	-0.20	-0.14	-0.18	-0.16	-0.25	-0.12	-0.29	-0.34	-0.34	-0.36	-0.29	-0.34
SST-2	0.00	-0.13	-0.30	0.00	0.19	-0.01	0.08	-0.22	-0.38	-0.09	0.05	-0.12
SST-3	0.00	0.01	0.04	0.14	0.33	0.17	0.11	0.08	0.11	0.21	0.25	0.27
SST-4	-0.08	-0.05	-0.03	0.09	0.11	0.08	0.08	0.04	0.02	0.05	0.09	0.15
SST-5	-0.43	-0.44	-0.31	-0.13	-0.08	-0.11	-0.11	-0.28	-0.35	-0.26	-0.16	-0.43

(c)

	Jan	Feb	Mar	Apr	May	June	July	Aug	Sep	Oct	Nov	Dec
DMI	-0.07	-0.25	-0.21	-0.11	-0.08	-0.03	-0.01	-0.10	-0.18	-0.22	-0.23	-0.19
SOI	-0.36	-0.33	-0.34	-0.14	0.08	0.18	0.01	0.19	0.24	0.15	0.18	0.37
SST-1	-0.14	0.07	0.28	0.31	0.20	0.26	0.15	0.20	0.14	0.15	0.10	-0.03
SST-2	0.14	0.16	0.00	-0.15	0.12	0.30	0.28	0.08	-0.07	-0.33	-0.22	-0.33
SST-3	0.35	0.40	0.47	0.43	0.41	0.26	0.23	0.19	0.12	-0.04	-0.10	-0.15
SST-4	0.00	-0.01	0.00	-0.02	-0.08	-0.10	-0.20	-0.22	-0.24	-0.32	-0.27	-0.23
SST-5	-0.15	-0.22	0.00	0.02	0.14	0.19	0.21	0.01	-0.05	-0.11	-0.14	-0.28

### 4.3.2 Rainfall Domain – TN West

On a contrary note, TN West domain mostly has significant correlations (at 95% confidence value) for short lag periods. In particular, the November rainfall (Table 4.8 (b)) in this domain is significantly correlated with the short lags of all the factors considered. While, October rainfall (Table 4.8 (a)) in this domain does not have any significant correlations, December rainfall (Table 4.8 (c)) is significantly correlated with only SST-3 values. It is interesting to note that SST-5 region has significant correlations with November rainfall in both TN East and TN West rainfall domains.

*Table 4.8 Time-lag Correlation matrices for TN West Rainfall Domain (a) October rainfall (b) November rainfall (c) December rainfall*

(a)

	Jan	Feb	Mar	Apr	May	June	July	Aug	Sep	Oct	Nov	Dec
DMI	0.09	0.18	0.19	0.19	0.11	0.03	0.04	0.06	0.06	0.06	0.08	0.07
SOI	0.05	0.26	-0.16	-0.08	-0.11	-0.12	0.01	-0.16	-0.31	-0.21	0.02	0.15
SST-1	0.00	-0.17	-0.07	0.10	0.07	0.02	-0.04	-0.12	-0.06	-0.10	0.02	-0.01
SST-2	0.23	0.16	0.21	0.17	-0.05	0.05	0.05	-0.10	0.07	-0.01	0.09	0.00
SST-3	-0.03	0.02	0.08	0.02	0.08	-0.01	0.03	0.00	0.00	0.09	0.13	0.10
SST-4	-0.15	-0.10	-0.03	0.02	0.02	0.08	0.11	0.09	0.13	0.17	0.18	0.13
SST-5	-0.03	-0.23	-0.09	0.04	0.10	-0.02	0.10	0.04	-0.04	0.04	0.06	0.17

(b)

	Jan	Feb	Mar	Apr	May	June	July	Aug	Sep	Oct	Nov	Dec
DMI	-0.03	-0.02	0.06	0.06	0.06	0.09	0.19	0.26	0.35	0.40	<b>0.49</b>	<b>0.57</b>
SOI	-0.20	0.11	-0.35	-0.37	-0.35	<b>-0.43</b>	-0.38	-0.38	<b>-0.41</b>	<b>-0.51</b>	-0.32	-0.38
SST-1	-0.26	-0.22	-0.10	0.09	0.18	0.28	-0.03	-0.06	-0.17	-0.31	<b>-0.46</b>	-0.12
SST-2	-0.18	-0.11	-0.04	-0.14	0.20	0.24	0.25	0.14	0.18	0.31	<b>0.58</b>	<b>0.57</b>
SST-3	0.10	0.19	0.30	0.37	<b>0.47</b>	<b>0.48</b>	<b>0.56</b>	<b>0.58</b>	<b>0.61</b>	<b>0.57</b>	<b>0.56</b>	<b>0.54</b>
SST-4	0.18	0.26	0.34	<b>0.49</b>	<b>0.46</b>	<b>0.46</b>	<b>0.50</b>	<b>0.42</b>	<b>0.42</b>	0.35	0.39	0.39
SST-5	-0.34	-0.11	0.06	0.04	0.13	0.08	0.08	-0.13	-0.11	-0.26	<b>-0.47</b>	-0.07

Table 4.8 (cont'd) Time-lag Correlation matrices for TN West Rainfall Domain (a) October rainfall (b) November rainfall (December rainfall)

(c)

	Jan	Feb	Mar	Apr	May	June	July	Aug	Sep	Oct	Nov	Dec
DMI	-0.03	-0.05	0.04	0.08	0.09	0.15	0.19	0.15	0.14	0.15	0.19	0.24
SOI	-0.21	-0.06	-0.27	-0.16	-0.21	-0.18	-0.12	0.07	0.08	0.03	0.19	0.26
SST-1	-0.16	-0.07	0.15	0.24	0.22	0.27	0.09	0.12	-0.02	-0.07	-0.20	-0.09
SST-2	0.07	0.04	0.11	0.01	0.22	0.23	0.27	0.31	0.32	0.08	0.19	0.07
SST-3	0.19	0.23	0.33	0.33	0.32	0.27	<i>0.40</i>	<b>0.46</b>	<b>0.43</b>	0.25	0.19	0.13
SST-4	0.03	0.04	0.02	0.05	-0.03	-0.02	-0.08	-0.08	-0.06	-0.15	-0.08	-0.11
SST-5	-0.16	-0.12	0.12	-0.06	0.18	0.19	0.08	0.03	-0.03	-0.25	<i>-0.37</i>	-0.28

#### 4.4 Principal Component Analysis and Regression model

PCA resulted in a set of eigenvalues and vectors for each rainfall domain, and those component loadings (elements of eigenvectors) that had eigenvalues of more than one were considered for further analysis. It was observed that three main factors, namely, SST-3, SST-5 and SST-2 (bolded out values in Table 4.9) had the highest component loadings irrespective of the rainfall domain in the order mentioned above. The higher the component loading value, the greater the variance explained by those factors. Thus, PCA resulted in a table of eigenvalues, component loadings for the top three eigenvalues, variance explained by these components (Table 4.10 (a)) and the percentage of total variance explained (Table 4.10 (b)) by each of these components. Ultimately, PCA has helped identify the main factors that statistically influence rainfall in the study region.

Table 4.9 Component Loadings for TN East Domain

Component Loadings			
	1	2	3
SST-3	<b>0.881</b>	0.211	0.041
SST-5	<b>0.792</b>	-0.388	-0.228
SST-2	<b>0.765</b>	-0.186	0.168
SST-1	0.726	-0.586	-0.200
DMI	0.205	0.721	0.370
SST-4	0.408	0.683	-0.384
SOI	-0.499	-0.647	0.102
TN East	-0.378	0.157	-0.773

Table 4.10 Variance explained by the first three components in TN East Domain (a) Total Variance explained (b) Percentage of Variance explained

(a)

Variance Explained by Components		
1	2	3
3.117	2.003	1.014

(b)

Percent of Total Variance Explained		
1	2	3
38.960	25.039	12.674

Table 4.11 Component Loadings for TN West Domain

Component Loadings			
	1	2	3
SST-3	<b>0.888</b>	0.181	-0.120
SST-5	<b>0.787</b>	-0.370	0.375
SST-2	<b>0.773</b>	-0.248	-0.378
SST-1	0.715	-0.586	0.238
SOI	-0.512	-0.627	0.061
DMI	0.206	0.718	-0.210
SST-4	0.437	0.687	0.249
TN West	-0.113	0.252	0.888

*Table 4.12 Variance explained by the first three components in TN West Domain (a) Total Variance explained (b) Percentage of Variance explained*

(a)

Variance Explained by Components		
1	2	3
3.025	2.018	1.254

(b)

Percent of Total Variance Explained		
1	2	3
37.809	25.224	15.672

Regression analysis was performed for each rainfall domain separately. The results ('R' output) are shown below. Although the p-value was very significant, the TN East model's coefficient of determination and F-statistic were not very high to be considered for further process of backward elimination. Thus, only TN West's model is concentrated here for further analysis and reference. The TN West model had both high significance and coefficient of determination as against the TN East model, thereby, leading to further analysis of the regression model. Backward elimination was carried out for TN West and was observed that both the initial and final models had SST-5 as one of the significant variables with good predictive power explaining rainfall variability.

## **TN West model**

### **1) Initial model**

`lm(formula = TNWest ~ SST1 + SST2 + SST3 + SST4 + SST5 + SOI + DMI, data = file)`

Residuals:

Min	1Q	Median	3Q	Max
-388.55	-128.50	-32.72	109.27	711.18

Coefficients:

	Estimate	Std.Error	tvalue	Pr(> t )	
(Intercept)	-3324.835	981.926	-3.386	0.001	***
SST1	18.690	47.889	0.390	0.697	
SST2	-212.446	25.544	-8.317	0.000	***
SST3	1.463	16.277	0.090	0.928	
SST4	89.811	21.992	4.084	0.000	***
SST5	220.501	46.644	4.727	0.000	***
SOI	46.902	15.104	3.105	0.002	**
DMI	47.615	17.554	2.713	0.007	**

---

Signif. codes: 0 '\*\*\*' 0.001 '\*\*' 0.01 '\*' 0.05 '.' 0.1 ' ' 1

Residual standard error: 208.1 on 280 degrees of freedom  
Multiple R-squared: 0.3578, Adjusted R-squared: 0.3417  
F-statistic: 22.28 on 7 and 280 DF, p-value: < 2.2e-16

## 2) Final model

lm(formula = TNWest ~ SST2 + SST4 + SST5 + SOI + DMI, data = file)

Residuals:

Min	1Q	Median	3Q	Max
-385.67	-128.78	-29.94	107.90	715.86

Coefficients:

	Estimate	Std.Error	tvalue	Pr(> t )	
(Intercept)	-3336.030	902.770	-3.695	0.000	***
SST2	-206.520	19.390	-10.649	0.000	***
SST4	89.830	21.710	4.137	0.000	***
SST5	234.840	31.010	7.572	0.000	***
SOI	45.730	13.540	3.378	0.001	***
DMI	43.580	13.130	3.319	0.001	**

---

Signif. codes: 0 '\*\*\*' 0.001 '\*\*' 0.01 '\*' 0.05 '.' 0.1 ' ' 1

Residual standard error: 207.4 on 282 degrees of freedom  
Multiple R-squared: 0.3574, Adjusted R-squared: 0.346  
F-statistic: 31.37 on 5 and 282 DF, p-value: < 2.2e-16

## CHAPTER 5

### DISCUSSION

#### 5.1 Time Series Analysis

This analysis enabled the comprehension of variations present within each phenomenon over the study period. As seen from the time series plots (Figure 4.5), both the TN East and TN West domains had evident seasonal cycles associated with their rainfall values which almost inhibited further analysis of these plots. This called for a monthly variation analysis which was best observed in box plots (Figure 4.6). As expected, the monthly variations were not uniform within the rainfall domains in TN. The TN East domain peaked mainly during the NEMR period, while the West domain peaked in June/July. This can be explained by the proximity of the TN West domain to the Western Ghats of South India which help bring SWMR in the months of June – September for most parts of the country (Revadekar and Kulkarni, 2008).

In accordance with the literatures about El-Nino (Bjerkness 1969, 1996; Kidson 1975), the time series plots of SST values in SST-3 and SST-4 and SOI values have complied with each other i.e. As mentioned earlier, SOI estimates the pressure difference between Tahiti and Darwin in East and West Pacific regions respectively and SST-3 and SST-4 regions' SST are measured in East and West Pacific regions respectively. Thus, high SST in SST-3 implies low SOI values and high SST in SST-4 implies high SOI values and vice versa. This is evident from the time series plots of these factors (Figures 4.8(c), 4.8(d) and 4.10(a)).

On a similar basis, the time series plots (Figures 4.8(a), 4.8(b) and 4.11(a)) of SST values in SST-1 and SST-2 and DMI values have conformed during this study period - i.e. high SST

values in Saji-East implies low DMI values and high SST values in Saji-West implies high DMI values. This effect is well manifested in these time series plots. Thus SSTs in the Saji areas are effective proxies for DMI changes, while also directly reflecting temperature changes.

Furthermore, it is interesting to note that SST-1 and SST-5 regions are significantly different from each other's SST values implying monitoring SST-5's values would help in the understanding of the physical processes occurring in this part of the Indian Ocean. This is of particular concern because the SST-5 region is geographically north of SST-1 but was not included as part of SST-1 (or Saji-East)'s boundary. Thus, it is suggested that SST-1's regional boundaries must be revisited and re-studied to demarcate a better SST region in the Eastern Indian Ocean than that of the current region.

## **5.2 Time-lag Correlation**

From time-lag correlations (Table 4.7, 4.8) it is evident that the TN East and TN West domains exhibited both similar and contrasting characteristics with respect to the various phenomena considered.

TN West exhibited significant correlations for the least possible lags; implying events occurring within a short duration (during the months of June, July, August, September) correlate more with the rainfall event peaking in November, than the events occurring far before the main rainfall event. This is in contradiction to TN East, which showed evidence of significant correlations with the highest possible lags. Thus, events occurring 7-10 months prior (during the months of January, February, March) have more significant correlations with November rainfall than that of events occurring right before the rainfall period.

Further, it is interesting to note that SST-5 has been observed to have significant correlations in each domain. These findings of lag-correlation analysis suggest a possibility of good correlation between the SST change before the earthquake event in December, 2004 and rainfall variation.

Additionally, it is noted that SST-1 and SST-2 do not have similar correlation trend across the domains. I.e. in TN East domain, SST-1 and SST-2 are significantly negatively correlated with NEMR November rainfall; In TN West, SST-1 is significantly negatively correlated while SST-2 is significantly positively correlated with NEMR November rainfall. This suggests the need for smaller rainfall domains than the state of Tamil Nadu, similar to what is done in the current research study.

With this in mind, it is important to refer to Geethalakshmi et. al., (2009) where it has been mentioned that SST-1 has positive correlation while SST-2 has negative correlation with Tamil Nadu's NEMR. This is contrary to the results above and to the correlation matrices. Not only are the results inconclusive but also is the correlation matrix (Table I in the article) is mistakenly wrong about the geographical boundaries of Saji-East and Saji-West regions in Geethalakshmi et al. (2009). This matrix has been referred by the article to support the result discussed in it. This, further, illustrates the need for a detailed analysis of the physical processes involved in the NEMR variability in Tamil Nadu that is not included in the current research study. Such a study would require a more complete representation of the synoptic scale circulations across the region. This could be done with regional climate models or intensive instrumentation combined with remote sensing.

In accordance with the literature, it is seen that SST-3 is positively correlated; SOI is negatively correlated with NEMR rainfall in all these domains (Geethalakshmi et. al., 2009). Although

time-lag correlation analysis helped in identifying the correlations among the factors, the variance explained by each of these factors needed to be thoroughly understood on an individual basis which was obtained from PCA component loadings.

### **5.3 Principal Component Analysis and Regression model**

Unlike time-lag correlation, PCA (Tables 4.9 - 4.12) results were similar for both the domains in TN with respect to the factors with highest component loadings. Irrespective of the domain, SST was found to lead the component loadings in comparison with the other factors, namely, DMI and SOI.

Furthermore, it was observed that SST-3, SST-5 and SST-2 had the highest possible component loadings value and, thus, highest variance explained in the above mentioned order. Approximately, first and second component loadings have accounted for 38% and 25% of total variance, respectively. It is seen that the total variance explained by the top three component loadings (with eigenvalues  $> 1$ ) for TN East domain is 76.7% and TN West domain is 78.7%.

Although it did not show up much in the time-lag correlation when compared to SST-3 and SST-2, the SST-5 region had the second largest PCA component loadings. Thus, PCA has narrowed down the original dataset to three main factors which explain the highest possible variance for rainfall pattern in TN with an emphasis of SST-5 being the second factor with highest variance. This suggests a possibility for the 2004 Earthquake epicenter region's SST values to have influence over TN rainfall variability. This should be validated with a physical or climate modeling experiment which is beyond the scope of the current research study.

As mentioned earlier, TN East's regression model did not have high significant coefficient of determination and F-statistic, leading to the concentration of TN West's regression model only. From backward elimination regression analysis approach, it was observed that SST-2, SST-4, SST-5, SOI and DMI significant variables were the final ones with good predictive power w.r.t. TN West's rainfall variability. Thus, SST-5 (the 2004 earthquake epicenter region, a new region proposed by this study) is one of the factors that have good causative power. It is quite surprising to note that SST-1 and SST-3 are eliminated from the final model because of their non-significant values. Although, the factors that are related to rainfall variability are identified, the physical mechanism behind this process is not known (yet) and/or analyzed by this study. This shortcoming is addressed in the limitations and conclusion sections of this document.

## **5.4 Limitations**

This study has several important limitations. First, more detailed analysis would have been possible had daily station rainfall values been made available instead of the daily interpolated (gridded) rainfall values over regular grids (0.5 degree latitude x 0.5 degree longitude). Despite the fact that input datasets are validated and evaluated against a standard dataset, the fact that interpolated datasets carry over a marginal uncertainty or error in each step should have affected this input dataset too.

Second this study has been entirely statistical in nature. Although this study has delved into various factors that affect rainfall variability in Tamil Nadu, the moisture transport (including convergence and divergence moisture flux) between the earthquake epicenter region and Tamil Nadu and physical process behind rainfall variability are still unknown. This could be made

possible with climate models which input/output various parameters to appreciate the physical process behind the scenes. But, in order to run such a climate model, a great deal of observational data is needed; the earthquake effect, if real, is likely a very small effect and may be difficult to segregate from natural rainfall variability. The physical processes involved here have merely helped address the issue of rainfall pattern predictability for this part of the globe.

## CHAPTER 6

### CONCLUSIONS

#### 6.1 Conclusions

This research study has, thus, focused on rainfall variability in TN with respect to SOI, DMI, and SST values over five main regions with main focus on the 2004 Earthquake Epicenter region. The general behavior of each phenomenon was comprehended from time series and variance analyses. This was followed by a Time-Lag Correlation, Principal Component Analysis and Regression model analysis of the phenomena. Based on these analyses, two significant rainfall domains in Tamil Nadu were identified. Second, SST was identified as the most dynamic variable of the dataset. Not only has PCA reported SST to be one of the main factors, but also it has suggested that the 2004 Earthquake epicenter region is the second most significant factor in this respect. Furthermore, SST-5 region is identified to be significantly correlated with rainfall in Tamil Nadu and has been observed to have significant predictive power over rainfall variability too. SST-1 and SST-5 are adjacent to each other, yet surprisingly different from each other both from ANOVA and PCA analyses. Even though, these two areas are close to each other, they are very different in their relationship to TN rainfall. This is a surprising result and needs to be analyzed in detail to investigate the physical processes in these regions.

Although, this study has identified correlated factors and their significance in explaining rainfall variability, the physical mechanism behind this variability is not tested in this project and, thus, not understood yet. It should be emphasized that this study has served and established the ground work necessary for comprehending such huge variations in Tamil Nadu. Further, it has not investigated the seismic activity reasoning which is beyond the scope of this project.

In order to understand the dominant climate modes better, this study could be extended to identify the wind pattern at various pressure levels between TN and Sumatra over the period of 24 years (1982 to 2005) and 2004 in particular. Although, the wind pattern would enable us to comprehend the movement of moisture laden clouds between the study regions, a thorough understanding would be made possible with ‘moisture transport study’ and ‘climate modeling’. Also, other local factors such as land use/land cover, urban heat islands, vegetation indices...etc. could be included for future analyses which would help recognize the rainfall variability completely. These components will form part of long term research goals to be accomplished in order to meticulously understand the rainfall pattern for Tamil Nadu, a South-Eastern state of India.

## **APPENDICES**

## R PROGRAMS

### R Program #1

# R routine to read \*.grd files

#Modified by Thulasi M. on 11/24/2010

```
readTime <- function(f,tm,x=69,y=65,size=4,type="double",NAvalue=-999){
  c = file(f,open="rb")
  seek(c,x*y*(tm-1)*size)
  m=matrix(readBin(c,type,x*y,size),x,y)
  #print(m)
  #print(dim(m))
  close(c)
  m[abs(m-NAvalue)<.Machine$double.eps] = NA
  m
  #print(m)
}
```

### R Program #2

# Extracts rainfall values for four chosen domains within TN region. They are TN East, TN West, TN North and TN South.

# Written by Thulasi M. on 12/20/2010

```
year <- c(1982:2005)
z <- c(1, 13, 25, 37, 49, 61, 73, 85, 97, 109, 121, 133, 145,
      157, 169, 181, 193, 205, 217, 229, 241, 253, 265, 277)
z1 <- c(0:11)

arr_e <- matrix(0, 288, 5)
colnames(arr_e) <- c("date", "min", "mean", "max", "IQR")
arr_w <- matrix(0, 288, 5)
colnames(arr_w) <- c("date", "min", "mean", "max", "IQR")
arr_nc <- matrix(0, 288, 5)
colnames(arr_nc) <- c("date", "min", "mean", "max", "IQR")
arr_s <- matrix(0, 288, 5)
colnames(arr_s) <- c("date", "min", "mean", "max", "IQR")

no.years <- 24

for (j in 1:no.years){

#non leap year loop
  if (year[j] %% 4){
    print(year[j])
    print("if (non-leap) loop is executed")
    days <- 365
    y <- c(0, 31, 59, 90, 120, 151, 181, 212, 243, 273, 304, 334, 365)
```

```

}    #if loop ends here

#leap year loop
else {
print(year[j])
print("else loop is executed")
days <- 366
y <- c(0, 31, 60, 91, 121, 152, 182, 213, 244, 274, 305, 335, 366)
}

e.x <- matrix(0, days, 4)
w.x <- matrix(0, days, 4)
nc.x <- matrix(0, days, 4)
s.x <- matrix(0, days, 4)

for(i in 1:days){
  file <- paste("F:/Maha/thesis/Datasets/RF_R/RF_data_R_0.5/rf0.5_", year[j], ".grd",
sep="")
  b <- readTime(file,i)
  e <- c(b[26, 9:14], b[27, 9:14])
  w <- c(b[20, 8:11], b[21, 7:8], b[22, 7:8])
  nc <- c(b[23, 9:14], b[24, 9:14], b[25, 9:14])
  s <- c(b[23, 4:6], b[24, 4:6])

  e.x[i, 1] <- min(e, na.rm=T)
  e.x[i, 2] <- mean(e, na.rm=T)
  e.x[i, 3] <- max(e, na.rm=T)
  e.x[i, 4] <- IQR(e, na.rm=T)

  w.x[i, 1] <- min(w, na.rm=T)
  w.x[i, 2] <- mean(w, na.rm=T)
  w.x[i, 3] <- max(w, na.rm=T)
  w.x[i, 4] <- IQR(w, na.rm=T)

  nc.x[i, 1] <- min(nc, na.rm=T)
  nc.x[i, 2] <- mean(nc, na.rm=T)
  nc.x[i, 3] <- max(nc, na.rm=T)
  nc.x[i, 4] <- IQR(nc, na.rm=T)

  s.x[i, 1] <- min(s, na.rm=T)
  s.x[i, 2] <- mean(s, na.rm=T)
  s.x[i, 3] <- max(s, na.rm=T)
  s.x[i, 4] <- IQR(s, na.rm=T)
}    #i loop ends here

```

```

months <- 12
for(k in 1:months){
  arr_e[z[j]+z1[k],1] <- paste(year[j], ".", k, sep="")
  arr_e[z[j]+z1[k],2] <-sum(e.x[(y[k]+1):y[k+1],1])
  arr_e[z[j]+z1[k],3] <-sum(e.x[(y[k]+1):y[k+1],2])
  arr_e[z[j]+z1[k],4] <-sum(e.x[(y[k]+1):y[k+1],3])
  arr_e[z[j]+z1[k],5] <-sum(e.x[(y[k]+1):y[k+1],4])

  arr_w[z[j]+z1[k],1] <- paste(year[j], ".", k, sep="")
  arr_w[z[j]+z1[k],2] <-sum(w.x[(y[k]+1):y[k+1],1])
  arr_w[z[j]+z1[k],3] <-sum(w.x[(y[k]+1):y[k+1],2])
  arr_w[z[j]+z1[k],4] <-sum(w.x[(y[k]+1):y[k+1],3])
  arr_w[z[j]+z1[k],5] <-sum(w.x[(y[k]+1):y[k+1],4])

  arr_nc[z[j]+z1[k],1] <- paste(year[j], ".", k, sep="")
  arr_nc[z[j]+z1[k],2] <-sum(nc.x[(y[k]+1):y[k+1],1])
  arr_nc[z[j]+z1[k],3] <-sum(nc.x[(y[k]+1):y[k+1],2])
  arr_nc[z[j]+z1[k],4] <-sum(nc.x[(y[k]+1):y[k+1],3])
  arr_nc[z[j]+z1[k],5] <-sum(nc.x[(y[k]+1):y[k+1],4])

  arr_s[z[j]+z1[k],1] <- paste(year[j], ".", k, sep="")
  arr_s[z[j]+z1[k],2] <-sum(s.x[(y[k]+1):y[k+1],1])
  arr_s[z[j]+z1[k],3] <-sum(s.x[(y[k]+1):y[k+1],2])
  arr_s[z[j]+z1[k],4] <-sum(s.x[(y[k]+1):y[k+1],3])
  arr_s[z[j]+z1[k],5] <-sum(s.x[(y[k]+1):y[k+1],4])
}   #k loop ends here

}   #j loop ends here

write.csv(arr_e, "mon_prec_sub_east.csv")
write.csv(arr_w, "mon_prec_sub_west.csv")
write.csv(arr_nc, "mon_prec_sub_center.csv")
write.csv(arr_s, "mon_prec_sub_south.csv")

```

### **R Program #3**

# This code extracts RF annual values for TN region and plots maps showing RF variations  
#within the study region. image.plot function is used to plot the 24-year rainfall mean for entire  
#TN region. Based on this plot and the rainfall values, 4 subsets, namely, Western, Eastern,  
#Central and Southern TN #regions are chosen.  
# Written by Thulasi M. on 12/17/2010

```

year <- c(1982:2005)
a <- array(0, c(69, 65, 24))
for (j in 1:24){
  for(i in 1:365){

```

```

file <- paste("F:/Maha/thesis/Datasets/RF_R/RF_data_R_0.5/rf0.5_", year[j], ".grd", sep="")
b <- readTime(file,i)
a[,j] <- a[,j] + b
}
}

#Color Ramp for the legend bar; easting and northing extent
aq.cols <- colorRampPalette(c("wheat4", "wheat", "light blue", "blue1", "blue4"))
x2 <- seq(76,len=11, by=0.5)
y2 <- seq(8, len=12, by=0.5)

# plots annual rainfall variations for each individual year starting 1982 to 2005
arr3 <- 0
for(i in 1:24){
arr2 <- a[20:30, 4:15, i]

#image plots for the individual year with legend bar
image.plot(arr2, x=x2, y=y2, col=aq.cols(10), xlab="Easting", ylab="Northing",
main=paste("Annual Rainfall Variations in Tamil Nadu, ", year[i]," (mm per year)", sep=""))
#contour(arr2, x=x2, y=y2, add=T)
im.out <- paste("Annual_RF_Var_", year[i], ".png", sep="")
dev.print(png, im.out, height=520, width=460)

arr3 <- arr3 + a[20:30, 4:15, i]
}

```

#### **R Program #4**

```

# This code extracts SST values from NetCDF file based on the lat/lon values mentioned.
#The final extracted values is for SST- 3 (El-Nino 3) region. Similarly, other SST regions are
#extracted.
#Written by Thulasi M. on 10/12/2010

```

```

library(ncdf)
library(RNetCDF)
library(chron)
library(zoo)
#library(date)

```

```

#####
# File Input #
#####

```

```

sst.nc <- open.ncdf("F:/Maha/thesis/Datasets/SST/sst.mnmean.nc")

```

```

#####
# Get data      #
#####

par(mfrow=c(2,3), ask=TRUE)
lat <- get.var.ncdf( sst.nc, "lat")      # coordinate variable
lon <- get.var.ncdf( sst.nc, "lon")      # coordinate variable
#z <- get.var.ncdf( sst.nc, "sst")      # variable (same as sst.nc$var)
v1.time <- get.var.ncdf(sst.nc, "time")
ex.time <- utcal.nc("days since 1800-1-1 00:00:00", v1.time)

#####
# Changed w.r.t sst.nc  #
# Start time - 12/1/1981 #
# End time - 12/1/2009  #
#####

v1 <- sst.nc$var[[1]]

#####
# Subset for El Nino-3 region
# all months from 1982 - 2008
# for all regions
#####
year <- 1982
month <- 1
day <- 1
for(i in 1982:2008){
  if (i == 1982) st.time <- which(ex.time[,1] == i & ex.time[,2] == 2 & ex.time[,3] == 1)
  else st.time <- which(ex.time[,1] == i & ex.time[,2] == 1 & ex.time[,3] == 1)
  end.time <- which(ex.time[,1] == i & ex.time[,2] == 12 & ex.time[,3] == 1)
  year <- c(year, ex.time[st.time:end.time])
  month <- c(month, ex.time[(st.time:end.time), 2])
  day <- c(day, ex.time[(st.time:end.time), 3])
}

len.y <- length(year)

data.e3 <- matrix(data=0, nrow=len.y, ncol=6,
  dimnames=list(1:len.y, c("year", "month", "min.sst.e3", "mean.sst.e3", "max.sst.e3",
  "IQR.sst.e3")))
for(j in 1:len.y) {
  st.time <- which(ex.time[,1] == year[j] & ex.time[,2] == month[j])
  start <- c(which(lon==210.5), which(lat==4.5), st.time)
  count <- c(length(which(lon==210.5):which(lon==269.5)),
  length(which(lat==4.5):which(lat==4.5)), 1)
}

```

```
data.e3[j,1] <- year[j]
data.e3[j,2] <- month[j]
data.e3[j,3] <- min(get.var.ncdf(sst.nc, v1, start=start, count=count))
data.e3[j,4] <- mean(get.var.ncdf(sst.nc, v1, start=start, count=count))
data.e3[j,5] <- max(get.var.ncdf(sst.nc, v1, start=start, count=count))
data.e3[j,6] <- IQR(get.var.ncdf(sst.nc, v1, start=start, count=count))
}
write.csv(data.e3, "F:/Maha/thesis/Datasets/SST/Data_SST_E3.csv")
```

## **REFERENCES**

## REFERENCES

- Allan, R. J., D. Chambers, et al. (2001). Is there an Indian Ocean dipole and is it independent of the El Nino-Southern Oscillation? Southampton, UK, International CLIVAR Project Office. **6**: 18-22.
- Ammon et. al., Rupture Process of the 2004 Sumatra-Andaman Earthquake, Science 2005
- Ashok, K., Z. Y. Guan, et al. (2001). "Impact of the Indian Ocean Dipole on the relationship between the Indian monsoon rainfall and ENSO." Geophysical Research Letters **28**(23): 4499-4502.
- Baquero-Bernal, A., M. Latif, et al. (2002). "On dipolelike variability of sea surface temperature in the tropical Indian Ocean." Journal of Climate **15**(11): 1358-1368.
- Behera, S. K., J. J. Luo, et al. (2006). "A CGCM study on the interaction between IOD and ENSO." Journal of Climate **19**(9): 1688-1705.
- Behera, S. K., P. S. Salvekar, et al. (2000). "Simulation of interannual SST variability in the tropical Indian Ocean." Journal of Climate **13**(19): 3487-3499.
- Behera, S. K. and T. Yamagata (2003). "Influence of the Indian Ocean Dipole on the southern oscillation." Journal of the Meteorological Society of Japan **81**(1): 169-177.
- Bjerknes, J. (1966). "A POSSIBLE RESPONSE OF ATMOSPHERIC HADLEY CIRCULATION TO EQUATORIAL ANOMALIES OF OCEAN TEMPERATURE." Tellus **18**(4): 820-&.
- Bjerknes, J. (1969). "ATMOSPHERIC TELECONNECTIONS FROM EQUATORIAL PACIFIC." Monthly Weather Review **97**(3): 163-&.
- Blanford, H. F. (1884). "On the Connexion of the Himalaya Snowfall with Dry Winds and Seasons of Drought in India." Proceedings of the Royal Society of London **37**: 3-22.
- Boos W. and Kuang Z. (2010). "Dominant control of the South Asian monsoon by orographic insulation versus plateau heating". Nature doi:10.1038/nature08707
- Dai, A., I. Y. Fung, et al. (1997). "Surface observed global land precipitation variations during 1900-88." Journal of Climate **10**(11): 2943-2962.
- Dey and R.P. Singh, Surface latent heat flux as an earthquake precursor, 2003
- Garcia E., PCA & SPCA Tutorial (2008) <http://www.miislita.com/information-retrieval-tutorial/pca-sPCA-tutorial.pdf>

Geethalakshmi, V., A. Yatagai, et al. (2009). "Impact of ENSO and the Indian Ocean Dipole on the north-east monsoon rainfall of Tamil Nadu State in India." Hydrological Processes **23**(4): 633-647.

Haddad, Z. S., J. P. Meagher, et al. (2004). "Global variability of precipitation according to the Tropical Rainfall Measuring Mission." Journal of Geophysical Research-Atmospheres **109**(D17): 7.

Hastenrath, S. (2002). "Dipoles, temperature gradients, and tropical climate anomalies." Bulletin of the American Meteorological Society **83**(5): 735-+.

Hocking R.R. (1976). "The analysis and selection of variables in linear regression". Biometrics **32**, 1-49.

Hotelling, H., Analysis of a complex of statistical variable into principal components; J. Educ. Psych., vol. 24, 417-441 (1933).

Iizuka, S., T. Matsuura, et al. (2000). "The Indian Ocean SST dipole simulated in a coupled general circulation model." Geophysical Research Letters **27**(20): 3369-3372.

Kidson, J. W. (1975). "TROPICAL EIGENVECTOR ANALYSIS AND SOUTHERN OSCILLATION." Monthly Weather Review **103**(3): 187-196.

Kripalani, R. H. and P. Kumar (2004). "Northeast monsoon rainfall variability over south peninsular India vis-a-vis the Indian Ocean dipole mode." International Journal of Climatology **24**(10): 1267-1282.

Kumar, K. K., B. Rajagopalan, et al. (1999). "On the weakening relationship between the Indian monsoon and ENSO." Science **284**(5423): 2156-2159.

Kumar, O., C. V. Naidu, et al. (2004). "Influence of southern oscillation and SSTs over Nino-3.4 region on the winter monsoon rainfall over coastal Andhra Pradesh." Proceedings of the Indian Academy of Sciences-Earth and Planetary Sciences **113**(3): 313-319.

Kumar, O. S. R. U. B., C. V. Naidu, et al. (2004). "Prediction of southern Indian winter monsoon rainfall from September local upper-air temperatures." Meteorological Applications **11**(3): 189-199.

Kumar, P., K. R. Kumar, et al. (2007). "On the recent strengthening of the relationship between ENSO and northeast monsoon rainfall over South Asia." Climate Dynamics **28**(6): 649-660.

Lay et. al., The Great Sumatra-Andaman Earthquake of 26 December 2004, Science, 2005

Meihua et. al., Surface latent heat flux anomalies prior to the Indonesia Mw 9.0 earthquake of 2004, Chinese Science Bulletin, 2006

Meyers G., et. al. (2006) "The Years of El Nino, La Nina and Interactions with the Tropical

Indian Ocean". *Journal of Climate* Vol. 20.

Normand, C. (1953). "MONSOON SEASONAL FORECASTING." *Quarterly Journal of the Royal Meteorological Society* **79**(342): 463-473.

Ouzounov et. al., Outlonging long wave radiation variability from IR satellite data prior to major earthquakes, *ScienceDirect*, 2006

Pant, G. and S. Parthasarathy (1981). "Some aspects of an association between the southern oscillation and indian summer monsoon." *Meteorology and Atmospheric Physics* **29**(3): 245-252.

Pant, G. B. and K. R. Kumar (1997). *Climates of South Asia*. Chichester, Wiley.

Parthasarathy, B. and G. B. Pant (1985). "SEASONAL RELATIONSHIPS BETWEEN INDIAN-SUMMER MONSOON RAINFALL AND THE SOUTHERN OSCILLATION." *Journal of Climatology* **5**(4): 369-378.

Rajeevan, M., Bhate, J., Kale, J.D. and B. Lal, 2006, High resolution daily gridded rainfall data for the Indian region: Analysis of break and active monsoon spells, *Current Science*, 91, 3, 296 – 306.

Rajeevan, M., J. Bhate, 2008 : "A high resolution daily gridded rainfall Data Set (1971-2005) for Mesoscale Meteorological Studies", NCC res. report no.9.

Rao, S. A., S. K. Behera, et al. (2002). "Interannual subsurface variability in the tropical Indian Ocean with a special emphasis on the Indian Ocean Dipole." *Deep Sea Research Part II: Topical Studies in Oceanography* **49**(7-8): 1549-1572.

Rasmusson, E. M. and T. H. Carpenter (1982). "VARIATIONS IN TROPICAL SEA-SURFACE TEMPERATURE AND SURFACE WIND FIELDS ASSOCIATED WITH THE SOUTHERN OSCILLATION EL-NINO." *Monthly Weather Review* **110**(5): 354-384.

Rasmusson, E. M. and T. H. Carpenter (1983). "The Relationship between Eastern Equatorial Pacific Sea-Surface Temperatures and Rainfall over India and Sri-Lanka." *Monthly Weather Review* **111**(3): 517-528.

Revadekar, J. V. and A. Kulkarni (2008). "The El Nino-Southern Oscillation and winter precipitation extremes over India." *International Journal of Climatology* **28**(11): 1445-1452.

Reynolds, R.W., N.A. Rayner, T.M. Smith, D.C. Stokes, and W. Wang, 2002: An improved in situ and satellite SST analysis for climate. *J. Climate*, 15, 1609-1625.

Roden, J., Trout, D., King, B.; A Tutorial on PCA Interpretation using CompClust (2005). [http://woldlab.caltech.edu/compclust/pca\\_interpretation\\_tutorial.pdf](http://woldlab.caltech.edu/compclust/pca_interpretation_tutorial.pdf)

- Ropelewski, C. F. and M. S. Halpert (1987). "Global and Regional Scale Precipitation Patterns Associated with the El-Nino Southern Oscillation." Monthly Weather Review **115**(8): 1606-1626.
- Ropelewski, C. F. and M. S. Halpert (1989). Precipitation Patterns Associated with the High Index Phase of the Southern Oscillation. **2**: 268-284.
- R.P. Singh et. al., Generic precursors to coastal earthquakes: Inferences from Denali fault earthquake, ScienceDirect, 2006
- R.P.Singh et. al., Multi-sensor studies of the Sumatra earthquake and tsunami of 26 December 2004, International Journal of Remote Sensing, 2007
- Saji, N. H., B. N. Goswami, et al. (1999). "A dipole mode in the tropical Indian Ocean." Nature **401**(6751): 360-363.
- Shearer and Burgmann, Lessons Learned from the 2004 Sumatra-Andaman Megathrust Rupture, Annual Review of Earth and Planetary Sciences 2010
- Shlens, J.; A tutorial on Principal Component Analysis: Derivation, Discussion and Singular Value Decomposition Technical report (2003) [http://www.cs.princeton.edu/picasso/mats/PCA-Tutorial-Intuition\\_jp.pdf](http://www.cs.princeton.edu/picasso/mats/PCA-Tutorial-Intuition_jp.pdf)
- Shukla, J. and D. A. Paolino (1983). "The Southern Oscillation and Long-Range Forecasting of the Summer Monsoon Rainfall over India." Monthly Weather Review **111**(9): 1830-1837.
- Sikka, D. (1980). "Some aspects of the large scale fluctuations of summer monsoon rainfall over India in relation to fluctuations in the planetary and regional scale circulation parameters." Journal of Earth System Science **89**(2): 179-195.
- Smith, L.; A tutorial on Principal Components Analysis; (2002). [http://www.cs.otago.ac.nz/cosc453/student\\_tutorials/principal\\_components.pdf](http://www.cs.otago.ac.nz/cosc453/student_tutorials/principal_components.pdf)
- Vaid, B. H., C. Gnanaseelan, et al. (2007). "Influence of pacific on southern indian ocean rossby waves." Pure and Applied Geophysics **164**(8-9): 1765-1785.
- Vinayachandran, P. N., S. Iizuka, et al. (2002). "Indian Ocean dipole mode events in an ocean general circulation model." Deep Sea Research Part II: Topical Studies in Oceanography **49**(7-8): 1573-1596.
- Walker, G. T. (1925). "CORRELATION IN SEASONAL VARIATIONS OF WEATHER" A FURTHER STUDY OF WORLD WEATHER1." Monthly Weather Review **53**(6): 252-254.
- Webster, P. J., A. M. Moore, et al. (1999). "Coupled ocean-atmosphere dynamics in the Indian Ocean during 1997-98." Nature **401**(6751): 356-360.

Yamagata, T., S. K. Behera, et al. (2003). "Comments on "Dipoles, temperature gradients, and tropical climate anomalies"." Bulletin of the American Meteorological Society **84**(10): 1418-1422.

Zubair, L. and C. F. Ropelewski (2006). "The strengthening relationship between ENSO and northeast monsoon rainfall over Sri Lanka and southern India." Journal of Climate **19**(8): 1567-1575.